# The Differentiation Stage of p53-Rb-deficient Bone Marrow Mesenchymal Stem Cells imposes the phenotype of *in vivo* sarcoma development

Ruth Rubio[1], Iván Gutierrez-Aranda[2], Ana I. Sáez-Castillo[2], Alberto Labarga[1], Michael Rosu-Myles[3], Sara Gonzalez-Garcia[4], Maria L Toribio[4], Pablo Menendez[1,6]*, and Rene Rodriguez[1,5]*

[1]Centre Pfizer-University of Granada-Andalusian Government for Genomics and Oncological Research (GENyO). [2]Andalusian Public Health System Biobank, Granada, Spain. [3]Centre for Vaccine Evaluation, Biologics and Genetic Therapies Directorate, Health Canada, Ottawa, Ontario, Canada. [4]Centro de Biología Molecular "Severo Ochoa" CSIC-UAM. Madrid. [5]Hospital Universitario Central de Asturias and Instituto Universitario de Oncología del Principado de Asturias, Oviedo, Spain. [6]Josep Carreras Leukemia Research Institute, Barcelona, Spain.

**Running Title:** Influence of the BM-MSC stage of differentiation in sarcoma development

**MS Character Count:** 5250

***Correspondence should be addressed to:**

Rene Rodriguez PhD
Hospital Universitario Central de Asturias and Instituto Universitario de Oncología del Principado de Asturias, Laboratorio 2 ORL–IUOPA, 33006 Oviedo, SPAIN.
Phone: 00 34 985 10 80 00 (ext 38524) / Fax: 00 34 985 10 80 15
Email: renerg@ficyt.es

Pablo Menendez PhD MBA
Center Pfizer-University of Granada-Andalusian Government for Genomics and Oncological Research (GENyO) / Josep Carreras Leukemia Research Institute.
Avda de la Ilustración 114. 18007. Granada / Facultat de Medicina. Carrer de Casanova 143 Barcelona. SPAIN.
Phone: 00 34 958 71 55 00 (ext 136) / Fax: 00 34 958 637 071
Email: pablo.menendez@genyo.es / pmenendez@carrerasresearch.org

**Pablo Menéndez and René Rodriguez share senior authorship*

**Authorship contributions:**

**R.Ru:** Conception and design, collection and/or of assembly data, data analysis, interpretation and manuscript writing. **S.G-G:** Collection of data, data analysis and interpretation **I.G-A, A.I.S, A.L, M.R-M, S.G-G & M.L.T:** Data analysis and interpretation. **P.M & R.Ro:** Conception and design, financial support, data analysis and interpretation and manuscript writing. The manuscript has been seen and approved by all authors.

**ABSTRACT**

Increasing evidence suggests that mesenchymal stem/stromal cells (MSCs) carrying specific mutations are at the origin of some sarcomas. We have reported that the deficiency of p53 alone or in combination with Rb ($Rb^{-/-}$ $p53^{-/-}$) in adipose-derived MSCs (ASCs) promotes leiomyosarcoma-like tumors *in vivo*. Here, we hypothesized that the source of MSCs and/or the cell differentiation stage could determine the phenotype of sarcoma development. To investigate whether there is a link between the source of MSCs and sarcoma phenotype, we generated $p53^{-/-}$ and $Rb^{-/-}p53^{-/-}$ MSCs from bone marrow (BM-MSCs). Both genotypes of BM-MSCs initiated leiomyosarcoma formation similar to $p53^{-/-}$ and $Rb^{-/-}p53^{-/-}$ ASCs. In addition, gene expression profiling revealed transcriptome similarities between p53- or Rb-p53-deficient BM-MSCs/ASCs and muscle-associated sarcomagenesis. These data suggest that the tissue source of MSC does not seem to determine the development of a particular sarcoma phenotype. To analyze whether the differentiation stage defines the sarcoma phenotype, BM-MSCs and ASCs were induced to differentiate towards the osteogenic lineage, and both p53 and Rb were excised using Cre-expressing adenovectors at different stages along osteogenic differentiation. Regardless the level of osteogenic commitment, the inactivation of Rb and p53 in BM-MSC-derived, but not in ASC-derived, osteogenic progenitors gave rise to osteosarcoma-like tumors which could be serially transplanted. This indicates that the osteogenic differentiation stage of BM-MSCs imposes the phenotype of *in vivo* sarcoma development, and that BM-MSC-derived osteogenic progenitors rather than undifferentiated BM-MSCs, undifferentiated ASCs or ASC-derived osteogenic progenitors, represent the cell of origin for osteosarcoma development.

**Keywords:** Mesenchymal stem cells; leiomyosarcoma; osteosarcoma; osteogenic differentiation; p53; Rb.

## INTRODUCTION

Multipotent mesenchymal stromal/stem cells (MSCs) represent a rare cell population present in many tissues that constitute a source of mesodermic progenitors (1). Increasing evidence suggests that MSCs might be the cell of origin or tumor-initiating cell capable of initiating sarcomagenesis, and several types of sarcomas have been modeled by inducing transformation of MSCs with different oncogenic events (2, 3). Sarcomas comprise a heterogeneous group of malignant tumors of mesenchymal origin that were historically grouped as soft tissue sarcomas (STS) and primary bone sarcomas (4). Sarcomas are generally studied once the full transformation events have already occurred, and therefore, the mechanisms of transformation are not amenable to analysis with patient samples, highlighting the need to establish *bona fide* experimental models to recapitulate sarcomagenesis. The development of *in vivo* sarcoma models using MSCs will likely constitute an unprecedented system to assay more efficient and specific therapies.

Dismantling of cell cycle regulation is often associated with sarcoma development (3). Indeed, alterations in *Rb* and *p53* genes are the most common mutations found in sarcomas characterized by complex kariotypes (i.e. osteosarcoma and leiomyosarcoma) (4). Furthermore, Li-Fraumeni syndrome, which is caused by germline p53 mutations, and patients with germline Rb mutations display a higher frequency of both osteosarcomas and STS (4, 5). In addition, the inactivation of the cell cycle control and the accumulation of genomic instability have been associated to spontaneous transformation of mouse MSCs (mMSCs) (6-9). Likewise, genetic targeting of *p53* in mMSCs triggers a transformation program in mMSCs (10-13).

p53 and Rb are master regulators of cell homeostasis controlling cell cycle, apoptosis, senescence, proliferation and differentiation. Regarding mesenchymal differentiation, p53

activation suppresses osteoblast differentiation by inhibiting the expression of Runx2 (14). Conversely, p53 deletion accelerates osteoblastic differentiation although impairs osteocyte terminal maturation (15). In addition to osteoblastic differentiation, p53 also inhibits the adipogenic and smooth muscle differentiation programs by down-regulating PPARγ and MYOCD, respectively (16). On the other hand, Rb has been reported to regulate mesenchymal differentiation along different mesenchymal lineages, including osteoblastic, adipogenic and myogenic through the transcriptional regulation of several lineage-specific transcription factors (17-20). For instance, Rb deficiency seems to impair bone development in favor of adipogenic differentiation (17, 19).

Mouse models displaying specific inactivation of p53 alone or in combination with Rb in the osteoblastic lineage through Oxterix-driven Cre expression developed osteoarcomas (21, 22). Similarly, another mouse model in which *p53* and *Rb* were inactivated in early mesenchymal tissues of embryonic limb buds also resulted in sarcoma development; mainly osteosarcomas although the concurrent deletion of *Rb* led to an increased prevalence of poorly differentiated STS (23). In contrast to these reports linking p53 and Rb deficiency with osteosarcoma development, we have previously reported that $p53^{-/-}$ and $p53^{-/-}Rb^{-/-}$ adipose-derived mesenchymal stem cells (ASCs) give rise to leiomyosarcoma-like tumors in immunedeficient mice, and in no case histopathological features of osteosarcoma were observed (13). Here, we hypothesize that there are two yet unexplored main factors potentially influencing the sarcoma phenotype, explaining at least in part, these differences between previous studies: (i) the distinct tissue source of the transformed MSCs and (ii) the different developmental stage along a particular mesenchymal lineage of the target cell in which transforming mutations arise. In order to address these two issues, MSCs were obtained from adipose tissue and BM from $p53^{loxP/loxP}$ and/or $Rb^{loxP/loxP}$ mice, and after Cre-mediated p53/Rb depletion, the tumorigenic potential of (i)

$p53^{-/-}$ and $Rb^{-/-}p53^{-/-}$ undifferentiated ASCs versus BM-MSCs and (ii) $Rb^{-/-}p53^{-/-}$ undifferentiated MSCs versus $Rb^{-/-}p53^{-/-}$ MSC-derived osteogenic progenitors was compared. Our data show that both $p53^{-/-}$ and $Rb^{-/-}p53^{-/-}$ undifferentiated BM-MSC and ASCs initiate leiomyosarcoma. On the other hand, the inactivation of Rb and p53 in BM-MSC-derived osteogenic progenitors give rise to osteosarcoma-like tumors serially transplantable in immunodeficient mice. In contrast, Rb and p53 deficiency in ASC-derived osteogenic progenitors fails to promote sarcomagenesis. These data indicate that: (i) the differentiation stage of the MSCs imposes the phenotype of *in vivo* sarcoma development, (ii) the osteogenic progenitors differentiated from MSCs from distinct tissue sources do not necessarily exhibit similar transformation potential, and (iii) BM-MSC-derived osteogenic progenitors rather than undifferentiated BM-MSCs, undifferentiated ASCs or ASC-derived osteogenic progenitors, seem to be the cell of origin for osteosarcoma development, at least when the cell cycle regulators Rb and p53 are deregulated.

## RESULTS

### *p53*$^{-/-}$ and *Rb*$^{-/-}$*p53*$^{-/-}$ deficient BM-MSCs give rise to leiomyiosarcoma in vivo

We have recently reported that the deficiency of p53 alone or in combination with Rb (Rb$^{-/-}$p53$^{-/-}$) in adipose-derived MSCs (ASCs) promotes leiomyosarcoma-like tumors *in vivo* (13). To determine whether there is a link between the tissue source of MSCs and sarcoma phenotype, we generated p53$^{-/-}$ and Rb$^{-/-}$p53$^{-/-}$ MSCs from bone marrow (BM-MSCs). BM-MSC cultures were successfully established from wt, Rb$^{loxP/loxP}$, p53$^{loxP/loxP}$ and Rb$^{loxP/loxP}$p53$^{loxP/loxP}$ mice. wt, Rb$^{-/-}$, p53$^{-/-}$ and Rb$^{-/-}$p53$^{-/-}$ BM-MSCs were generated by excision of loxP sequences using *Cre-recombinase*-expressing adenoviral vectors (Ad-CMV-Cre) (**Fig. 1A**). Depletion of Rb and/or p53 in BM-MSCs was confirmed by genomic PCR (**Fig. 1B**) and Western blot (**Fig. 1C**). As expected, the expression of both Rb and p53 was increased upon treatment with the topoisomerase I inhibitor campthotecin. BM-MSC cultures, similar to ASC cultures (13) showed typical mesenchymal surface antigen phenotype regardless of the genotype (**Fig. S1A**). Functionally, p53$^{-/-}$, and especially Rb$^{-/-}$p53$^{-/-}$ BM-MSCs displayed a reduced adipogenic differentiation potential whereas the osteogenic capacity was enhanced in Rb$^{-/-}$p53$^{-/-}$ BM-MSCs (**Fig. S1B**).

To assay the *in vivo* tumorigenic potential of the different BM-MSC genotypes, NOD/SCID IL2Rγ$^{-/-}$ mice were inoculated subcutaneously (s.c.) with either wt, Rb$^{-/-}$, p53$^{-/-}$ and Rb$^{-/-}$p53$^{-/-}$ BM-MSCs. Identical to the results obtained with p53$^{-/-}$ and Rb$^{-/-}$p53$^{-/-}$ ASCs (13), p53$^{-/-}$ and Rb$^{-/-}$p53$^{-/-}$ BM-MSCs, but not wt and Rb$^{-/-}$ BM-MSCs developed tumors *in vivo* (**Table 1**). Tumors arising from Rb$^{-/-}$p53$^{-/-}$ BM-MSCs displayed a higher penetrance (75% vs 50%) and a significantly shorter latency (65 *vs* 107 days) than tumors generated from p53$^{-/-}$ BM-MSCs (**Table 1 & Fig. 1D**). Histological analysis classified these tumors as leiomyosarcomas-like tumors as they displayed key features of these smooth muscle-related tumors such as fascicles of cells intersecting at ~90º, elongated cells showing hiperchromatosis and pleomorfism in nuclei and isolated

multinucleated giant cells. More importantly, $p53^{-/-}$ and $Rb^{-/-}p53^{-/-}$ derived tumors stained positive for smooth muscle-specific markers such as α-smooth muscle actin (SMA) and caldesmon but were negative for skeletal muscle markers such as myosin (**Figure 1E**). Together, $p53^{-/-}$ and $Rb^{-/-}p53^{-/-}$ deficient BM-MSCs initiate leiomyosarcoma formation similar to $p53^{-/-}$ and $Rb^{-/-}p53^{-/-}$ ASCs (**Fig. S2**). This suggests that at least in the context of deregulation of the cell cycle regulators *Rb* and *p53*, the tissue source of undifferentiated MSC does not seem to determine the phenotype of sarcoma development *in vivo*.

To further characterize these experimentally induced leiomyosarcomas, primary tumors derived from $p53^{-/-}$ (n=3) and $Rb^{-/-}p53^{-/-}$ (n=3) BM-MSCs were mechanically disaggregated and placed back in MSC culture conditions to establish immortalized cell lines (TBM-p53-1 to -3 and TBM-Rbp53-1 to -3). As expected, these tumor-derived cell lines remained deficient for p53 and Rb (**Fig. S3A**) and displayed identical morphology and immunophenotype to the parental BM-MSCs (data not shown). To investigate their tumorigenic potential, one of these *ex* vivo-established cell lines were inoculated s.c. into secondary immunodeficient mice. All mice transplanted with either TBMp53 or TBMRbp53 cell lines developed tumors with a 100% penetrance and a much shorter latency period (~2 weeks) than the primary tumors (**Fig. S3B**). Histopathological analysis of these tumors revealed that they retained the morphology and phenotype of leiomyosarcoma, including the expression of the SMA and caldesmon (**Fig. S3C**). These data demonstrate that the leiomyosarcoma tumors can be serially transplanted, indicating the presence of leiomyosarcoma-initiating cells within the $p53^{-/-}$ and $Rb^{-/-}p53^{-/-}$ undifferentiated BM-MSC cultures.

**Gene expression analysis supports that p53- or Rbp53-deficiency in both BM-MSCs and ASCs promotes muscle-associated sarcomagenesis**

Regardless the tissue of origin (BM or fat), $p53^{-/-}$ and $Rb^{-/-}p53^{-/-}$ deficient MSCs initiate leiomyosarcoma *in vivo*, as confirmed by histology analysis (**Fig. 1E & Fig. S2**). We then undertook gene expression profiling (GEP) in primary $p53^{-/-}$ and $Rb^{-/-}p53^{-/-}$ BM-MSCs and ASCs as well as in their *ex vivo*-derived tumoral $p53^{-/-}$ (Tp53) and $Rb^{-/-}p53^{-/-}$ (TRbp53) cell lines to analyze the gene expression signature and determine whether these signatures may partially mirror a particular type of sarcoma. Lists of genes differentially expressed (p-value<0.05; expression > 2-fold up or down) between the different cell types and their corresponding wt controls (wt-ASCs or wt-BM-MSCs) were generated. Using the IPA Software we searched for biological functions significantly altered with special focus on cancer. Among the genes differentially altered in $p53^{-/-}$ and $Rb^{-/-}p53^{-/-}$ deficient cells, we selected those classified by the IPA software as "sarcoma-related". Intriguingly, genes differentially expressed (as compared to wt) in $p53^{-/-}$- and $Rb^{-/-}p53^{-/-}$- deficient primary or tumoral cells, independent of their origin -BM or adipose tissue- were mainly grouped by the IPA software as muscle-associated sarcomas (myosarcoma, leiomyosarcoma, leiomyomatosis, tumorogenesis of the muscle or rhabdomyosarcoma) and no differentially expressed genes were clustered as associated to other type of sarcoma (osteosarcoma, liposarcoma, chondrosarcoma, etc) (**Fig. 2A & Fig. S4**).

We next compared the gene expression signature of tumoral Tp53 cells derived from $p53^{-/-}$ ASC *versus* $p53^{-/-}$ BM-MSCs and found that they shared 41%-62% of the genes differentially expressed (**Fig. 2B**). Similar overlap (39%-58%) was found between the TRbp53 derived from $Rb^{-/-}p53^{-/-}$ ASC and $Rb^{-/-}p53^{-/-}$ BM-MSCs (**Fig. 2B**). This large overlay in the transcriptional profiling molecularly supports that p53- or Rbp53-deficiency in both undifferentiated BM-MSCs and ASCs promotes similar leiomyosarcoma *in vivo*.

Finally, in order to gain insights into the signaling pathways which may be contributing to the development of leiomyosarcoma, we selected those genes commonly altered in Tp53 and TRbp53 cells that were associated to leiomyosarcoma by the IPA software. We found few genes exclusively altered in either Tp53 or TRbp53 cells (**Fig. 2C**). In contrast, the majority of genes were commonly altered in both Tp53 and TRbp53 cells (**Fig. 2C**), affecting key signaling pathways such as NF-kB pathway, PTEN signaling, IL-8 signaling and PI3K/AKT signaling (**Fig. 2C**). Therefore, the deregulation of these signaling pathways could be on the basis of the leiomyosarcoma pathogenesis in our experimental tumoral models.

**Depletion of Rb and p53 in BM-MSC-osteogenic derivatives leads to osteosarcoma development *in vivo***

The tissue source of MSC does not seem to determine the phenotype of sarcoma development *in vivo* as suggested by the fact that Rb and p53 deficiency in undifferentiated ASC or BM-MSCs give rise to the same tumor -leiomyosarcoma-. However, we hypothesized that the cell of origin for osteosarcomas could be an osteogenic lineage-committed progenitor cell rather than undifferentiated MSCs, and that the same oncogenic events might trigger different sarcoma phenotype depending on the differentiation/developmental stage of the MSCs being targeted. Thus, to analyse whether the BM-MSC/ASC differentiation stage may define the sarcoma phenotype, $Rb^{loxP/loxP}p53^{loxP/loxP}$ BM-MSCs/ASCs were induced to differentiate towards the osteogenic lineage and both *Rb* and *p53* were excised using Ad-CMV-Cre at different stages [day 0 (BM/ASC-Rbp53-Undiff cells), 2 (BM/ASC-Rbp53-2Days cells), 5 (BM/ASC-Rbp53-5Days cells) and 10 BM/ASC-Rbp53-10Days cells)] along the osteogenic differentiation (**Fig. 3A**).

Depletion of Rb and p53 in undifferentiated BM-MSCs/ASCs and their osteogenic derivatives was confirmed by genomic PCR (**Fig. 3B**). Gradual *in vitro* osteogenic differentiation was monitored

by q-RT-PCR analysis for several master osteogenic-specific factors such as osterix, BMP4, osteopontin, collagen type I and osteocalcin (**Fig. 3C**). Likewise, proper osteogenic differentiation was functionally confirmed through the detection of osteogenic-associated calcium deposition by Alizarin red staining (**Fig. 3D**).

The tumorigenic potential of Rb and p53 depletion after 0, 2, 5 and 10 days of osteogenic differentiation was assessed by s.c. inoculation into NOD/SCID IL2Rγ$^{-/-}$ mice. All Rb$^{-/-}$p53$^{-/-}$ BM-MSCs initiated tumors *in vivo* regardless their stage of differentation with similar incidence (between 70% and 80%) and latency (ranging from 62 to 68 days) (**Table 2 & Fig 4A**). As expected, BM-Rbp53-Undiff cells initiated leiomyosarcoma-like tumors (**Fig. 1 & Fig. 4B**). However, tumors formed by BM-Rbp53-2Days, BM-Rbp53-5Days or BM-Rbp53-10Days cells consistently displayed clear osteosarcoma histological features including widespread areas of eosinophilic osteoid material containing cells embedded into the matrix as well as some areas of well-formed bone (**Fig. 4B**).

To determine whether these experimentally induced osteosarcomas can be serially transplanted, primary tumors formed from BM-Rbp53-2Days or BM-Rbp53-10Days cells as well as from BM-Rbp53-Undiff cells were mechanically disaggregated and placed back in MSC culture conditions to establish immortalized cell lines (TBM-Rbp53-2Days, TBM-Rbp53-10Days and TBM-Rbp53-Undiff). As expected, these tumor-derived cell lines remained deficient for Rb and p53 (**Fig. S5A**). All the cell lines were able to generate tumors *in vivo* with a 100% penetrance and with a short latency period of 18-35 days (**Fig. S5B**). Histopathological analysis of the secondary tumors generated from TBM-Rbp53-2Days and TBM-Rbp53-10Days revealed that they retained the main features of primary osteosarcomas including the presence of large areas of osteoid matrix whereas the secondary tumors derived from TBM-Rbp53-Undiff retained the leiomyosarcoma

phenotype (**Fig. S5B**). This data demonstrates that the osteosarcoma-like phenotype can be serially transplanted, indicating the presence of osteosarcoma-initiating cells within the $Rb^{-/-}p53^{-/-}$ BM-MSC-derived osteogenic progenitors.

Remarkably, Rb and p53 depletion in more committed osteogenic derivatives formed osteosarcoma-like tumors with more differentiated structures than in less differentiated osteogenic derivatives (**Fig. 4B**). Thus, osteosarcomas formed by BM-Rbp53-2Days cells or BM-Rbp53-5Days presented areas of osteoid matrix that became much denser in tumors formed by BM-Rbp53-10Days cells where areas of immature well-formed bone were eventually commonly developed (**Fig. 4B**). This observation is supported by the quantification of osteoid areas in randomly taken pictures from 3 different tumors of each condition. The presence of osteoid matrix in tumors developed from BM-Rbp53-10Days cells was 2-fold larger than in the tumors formed by BM-Rbp53-2Days or BM-Rbp53-5Days cells (**Fig 4C**). Furthermore, the early osteogenic transcription factor Osterix was specifically up-regulated in the tumoral cell lines TBM-Rbp53-2Days and TBM-Rbp53-5Days whereas the late osteogenic marker osteocalcin was exclusively up-regulated in the tumoral cell line TBM-Rbp53-10Days, indicating a higher degree of differentiation (**Fig 4D**). Altogether, this data suggests that the differentiation stage of BM-MSCs imposes the phenotype of *in vivo* sarcoma development.

On the other hand, none of the $Rb^{-/-}p53^{-/-}$ ASC-derived osteogenic progenitors developed tumors when inoculated into NOD/SCID IL2Rγ$^{-/-}$ mice (**Table 2**) and only the ASC-Rbp53-Undiff cells gave rise to leimyosarcoma-like tumors *in vivo* (**Table 2 and Fig. 2S**). These data indicate that the osteogenic progenitors differentiated from MSCs from distinct tissue sources do not necessarily exhibit similar transformation potential, and that BM-MSC-derived osteogenic progenitors rather than undifferentiated BM-MSCs, undifferentiated ASCs or ASC-derived

osteogenic progenitors, seem to be the cell of origin for osteosarcoma development, at least when the cell cycle regulators Rb and p53 are depleted.

**Gene expression analysis supports that Rb and p53 inactivation in BM-MSCs but not ASC-derived osteogenic progenitors promotes osteosarcoma development.**

To deepen our molecular understanding about the different tumor formation ability of BM-MSC- and ASC-derived osteogenic progenitors we undertook GEP in BM- and ASC-Rbp53-10Days cells as well as in the *ex vivo*-derived tumoral TBM-Rbp53-10Days cells. IPA analysis of the lists of genes differentially expressed as compared to wt controls (wt-ASCs or wt-BM-MSCs) showed that the ASC-Rbp53-10Days cells were mainly associated with muscle-related sarcomas despite osteogenic priming (**Fig 5A & Fig S6**), similarly to ASC-Rbp53-Undiff cells (**Fig 2A**). However, although IPA analysis showed a poor selection of genes related with sarcomas in BM-Rbp53-10Days it revealed many genes associated to bone cancer and osteosarcoma in TBM-Rbp53-10Days tumoral cells **(Fig 5A & FigS6)**, confirming the histological diagnosis of these tumors.

The gene expression signature of ASC-Rbp53-10Days and BM-Rbp53-10Days cells displayed an overlap of 27-29% (**Fig. 5B**), which is much lower than that observed between the tumors developed from the corresponding undifferentiated cells (**Fig 2B**). This different gene expression signature between ASC-Rbp53-10Days and BM-Rbp53-10Days cells might partially explain the distinct tumor formation ability of the BM-MSC- and ASC-derived osteogenic progenitors. Using the IPA software, the signaling pathways and upstream regulators signalling associated to the group of genes specifically altered in ASC-Rbp53-10Days cells (left column) and in BM-Rbp53-10Days cells (right column) were analyzed (**Fig. 5C**). The pathways and upstream regulators signalling most significantly altered in the ASCs-Rbp53-10Days cells are mainly related with cell cycle control and DNA repair, whereas many of those altered in the BM-Rbp53-10Days cells are

related to cell fate signaling, including several pathways involved in osteogenic differentiation and/or osteosarcoma development, including WNT-β-catenin, BMP-TGFβ or calcium signaling pathways (24). While alterations in cell cycle regulation are common in osteosarcoma, the lack of alteration in WNT/β-catenin or BMP-TGFβ signaling pathways which are highly related to osteosarcoma development could partially explain the inability to initiate osteosarcoma of Rb and p53 deficient ASC-derived progenitors.

## DISCUSSION

Increasing evidence suggests that MSCs carrying specific mutations may be at the origin of sarcomas. Accordingly, modelling sarcomagenesis using MSCs is becoming an active area of research in an attempt to develop better sarcoma models to deepen our understanding about the cellular and molecular mechanisms underlying sarcoma initiation and pathogenesis (2, 3). Mutations that contribute to tumoral transformation often disrupt cellular growth/survival by dismantling cell cycle checkpoints, and alterations in cell cycle regulators are frequent in sarcomas. In fact, we have recently reported that the deficiency of p53 alone or in combination with Rb ($Rb^{-/-}$ $p53^{-/-}$) in adipose-derived MSCs (ASCs) promotes leiomyosarcoma-like tumors *in vivo*. However, to what extent the source of MSCs and the MSC differentiation stage influence the phenotype of sarcoma development remain to be elucidated.

In order to address these issues, the tumorigenic potential of (i) $Rb^{-/-}$, $p53^{-/-}$ and $Rb^{-/-}p53^{-/-}$ undifferentiated ASCs versus BM-MSCs and (ii) $Rb^{-/-}p53^{-/-}$ undifferentiated BM-MSCs/ASCs *vs* $Rb^{-/-}p53^{-/-}$ BM-MSC/ASC-derived osteogenic progenitors was compared. $p53^{-/-}$ and $Rb^{-/-}p53^{-/-}$ BM-MSCs initiated leiomyosarcoma upon inoculation in immunedeficient mice with similar latency and incidence to $p53^{-/-}$ and $Rb^{-/-}p53^{-/-}$ ASCs, indicating that the source of MSC does not seem to play a major role in defining the phenotype of sarcoma development *in vivo*. Nevertheless, we cannot rule out the possibility that MSCs from other tissues, targeted for Rb and p53 or other transforming mutations, would trigger different sarcomagenic programs.

The potential MSC origin of leiomyosarcoma is supported by a differentiation-based microRNA study (25). Likewise, the deficiency of p53 and Rb in dermal MSCs was associated with the formation of pleomorphic STS (26). In this study, 33% of the STS developed in the $p53^{loxP/loxP}$ mice treated with Cre-expresing adenovectors were classified as pleomorphic leiomyosarcomas.

In other mouse models in which mutations are restricted to muscle, p53 deficiency cooperated with oncogenic K-RAS to induce the formation of high grade sarcomas with myofibroblastic differentiation (27). Similarly, the deficiency in p53 and Rb has also been linked to leiomyosarcoma development in mouse ovaries (28). Altogether, p53 and Rb deficiency in undifferentiated MSCs of different tissue origin imposes leiomyosarcoma development. The analysis of gene expression signatures in primary $p53^{-/-}$ and $Rb^{-/-}p53^{-/-}$ BM-MSCs and ASCs as well as in their *ex vivo*-established tumoral cell lines (Tp53 and TRbp53) showed a large overlap between BM and fat models and supported that Rb and p53 deficiency is associated to muscle-associated sarcomagenesis, regardless the tissue origin of the MSCs (**Fig. 2A-B**). Using IPA software we selected those genes commonly altered in Tp53 and TRbp53 cells that were defined in public databases as associated to leiomyosarcoma (**Fig. 2C**). A high proportion of genes (40-60%) were commonly altered in both Tp53 and TRbp53 cells affecting key signaling pathways such as NF-kB pathway, PTEN signaling, IL-8 signaling and PI3K/AKT signaling. Interestingly, it has been reported that PTEN and AKT-mTOR pathways play a critical role in the development of leiomyosarcomas (29). Despite being well-established cancer-related pathways, the NFκB and IL-8 signaling pathways remain unexplored in leiomyosarcoma. Therefore, the deregulation of these signaling pathways could be on the basis of the leiomyosarcoma pathogenesis in our experimental tumoral models.

To analyze whether the differentiation stage may impose the sarcoma phenotype, BM-MSCs were induced to differentiate towards the osteogenic lineage and both p53 and Rb were excised using Cre-expressing adenovectors at different stages (day 2, 5 and 10) along osteogenic differentiation. Opposite to undifferentiated $Rb^{-/-}p53^{-/-}$ BM-MSCs, $Rb^{-/-}p53^{-/-}$ BM-MSC-derived osteogenic progenitors developed osteosarcoma-like tumors. Importantly, the longer the MSCs were allowed to differentiate towards osteogenic lineage the more differentiated osteosarcomas

developed (**Fig. 4B-D**). Moreover, primary osteosarcomas were capable of reproducing the tumor phenotype in a secondary transplantation round, suggesting the presence of osteosarcoma-initiating cells. These data suggest that the osteogenic differentiation stage of BM-MSCs imposes the phenotype of *in vivo* sarcoma development, and that BM-MSC-derived osteogenic progenitors rather than undifferentiated BM-MSCs may represent the cell of origin in osteosarcoma. Our results are in line with previous reported mouse models in which p53 and Rb were specifically inactivated in the osteoblastic lineage by expressing Cre-recombinase under the regulation of the Osterix1 promoter (21, 22). In these studies, osteosarcoma development was dependent on the loss of p53 and a concomitant loss of Rb accelerated tumorogenesis. Similarly, other mouse models in which *p53* and *Rb* were inactivated in early mesenchymal tissues of embryonic limb buds after the expression of Cre-recombinase under the regulation of the Prx1 promoter also resulted in osteosarcoma development although the concurrent deletion of *Rb* led to an increased prevalence of poorly differentiated STS (23) and hibernomas (17). However, the interpretation of sarcomagenesis models based on early mesenchymal tissue become somehow complicated given that the majority of human STS affects adults. The absence of a promoter capable of specifically driving Cre-recombinase expression in adult undifferentiated MSC poses a challenge for using similar mouse models to determine which tumor phenotype results upon *in vivo* specific inactivation of p53 and Rb in adult undifferentiated MSC. However, our *ex vivo* $Rb^{-/-}p53^{-/-}$ model has successfully allowed to compare the sarcoma phenotype upon inactivation of *p53* and *Rb* both in undifferentiated MSCs and in MSC-derived osteogenic progenitors. Importantly, although *Rb* and *p53* inactivation in undifferentiated BM-MSCs did not initiate osteosarcoma, it cannot be ruled out that alternative mutations could induce osteosarcoma development in undifferentiated BM-MSCs. For instance, aneuploidization and the genomic loss of CDKN2A/p16 in BM-MSCs (8, 9) or the expression of c-MYC in $p16^{INK4A-/-}p19^{ARF-/-}$ BM-MSCs resulted in osteosarcoma development (30). Importantly, it has been reported that loss of functional INK4A/ARF locus has a

critical role in the development of human osteosarcoma (31, 32). Thus, CDKN2A/p16 could be altering the differentiation programs of undifferentiated MSCs. In this line, in the c-MYC-p16$^{INK4A-/-}$ p19$^{ARF-/-}$ model (30), the cell population presenting a higher ability to form osteosarcoma has lost the adipogenic potential in favor of the osteogenic potential, suggesting that the cell of origin for osteosarcoma may be a MSC population that have lost/reduced the adipogenic potential. Accordingly, our *in vitro* differentiation data support a reduced adipogenic differentiation coupled to an increased osteogenic potential of Rb$^{-/-}$p53$^{-/-}$ BM-MSCs (**Fig. 1SB**).

Interestingly, the development of osteosarcoma-like tumors occurs when *Rb* and *p53* are targeted specifically in BM-MSC osteogenic derivatives as demonstrated by the fact that Rb$^{-/-}$p53$^{-/-}$ ASC-derived osteogenic derivatives did not develop sarcoma when inoculated into NOD/SCID IL2Rγ$^{-/-}$ mice, indicating that the osteogenic progenitors differentiated from MSCs from distinct tissue sources do not necessarily exhibit similar transformation potential. Accordingly, the gene expression signature of Rb$^{-/-}$p53$^{-/-}$ BM-MSC and ASC-derived osteogenic progenitors is considerably different with only ~28% overlap (**Fig 5B**). The osteosarcoma related WNT/β-catenin and BMP-TGFβ pathways are associated to the group of genes altered in BM-Rbp53-10Days cells but not in ASC-Rbp53-10Days cells, likely contributing to the different sarcomagenic potential (24) (**Fig 5C**). This distinct potential may be closely related to the differences revealed in the *in vivo* differentiation potential of MSCs derived from BM and other tissue sources (33). These leiomyosarcoma/osteosarcoma models based on p53 and Rb depletion in undifferentiated MSC or MSC-derived osteogenic progenitors make us to speculate, in a global context, that a particular set of oncogenic mutations may impose one sarcoma phenotype or other, depending on the differentiation stage partially influenced by the tissue source.

Our data based on *ex vivo* MSCs extends our current knowledge about the cell of origin, the influence of the source and the differentiation stage of MSCs, and *p53* and *Rb* deficiency in the phenotype of *in vivo* sarcoma development. In summary we show that: (i) p53 deficiency is sufficient to transform both BM-MSCs and ASCs; (ii) Rb deficiency on its own is not sufficient to transform MSCs, but it potentiates sarcomagenesis induced by p53 inactivation; (iii) both $Rb^{-/-}$ $p53^{-/-}$ undifferentiated BM-MSCs and ASCs initiate leiomyosarcoma *in vivo*; (iv) the osteogenic differentiation stage of BM-MSCs influences the phenotype of *in vivo* sarcoma development; (v) the cell of origin of osteosarcoma seems to be a BM-MSC-derived osteogenic progenitor rather than undifferentiated BM-MSCs, undifferentiated ASCs or ASC-derived osteogenic progenitors.

## MATERIAL AND METHODS

### Generation of mutant MSCs

MSCs were obtained from adipose tissue from gonadal, retroperitoneal and subcutaneous depots (ASCs) as previously described (11, 13) and from BM (BM-MSCs) of FVB background mice bearing alleles for either *p53*, *Rb* or both genes flanked by LoxP sites (13, 34). BM cells were flushed from the BM using a syringe with complete MSC growth medium (DMEM-Advanced, 10% FBS, 1% Pen/Strep and 1% Glutamax, all from Gibco). The cell suspension obtained was passed through a 70μm nylon filter (Becton Dickinson Biosciences, San Jose, CA), washed twice and seeded at a density of 25 x $10^6$ cells/$cm^2$ in MesenCult medium (Stem Cell Technologies, Vancouver, Canada) at 37ºC in a 5% $CO_2$ humidified atmosphere. After 24h, non-adherent cells were discarded and fresh medium was added. BM-MSC cultures were established from four mouse strains: (a) wt, (b) $Rb^{loxP/loxP}$, (c) $p53^{loxP/loxP}$ and (d) $p53^{loxP/loxP}$ $Rb^{loxP/loxP}$. Mutant BM-MSCs were generated by excision of the LoxP-flanked sequences by infection of all MSC cultures with adenoviral vectors expressing the Cre-recombinase gene under the control of the CMV promoter (Ad-CMV-Cre) (13). Successful gene knockdown and subsequent generation of $p53^{-/-}$, $Rb^{-/-}$ and $p53^{-/-}Rb^{-/-}$ MSC cultures after the excision of the LoxP regions was confirmed by genomic PCR and western blot. Only cells between passages 5 and 15 were used from downstream experiments.

### Genomic PCR

Total DNA was extracted using the DNAeasy kit (Qiagen, Alameda, CA). 200 ng of DNA were used for each PCR reaction. PCR conditions were as follows: pre-denaturation at 94ºC for 5 mins followed by 29 cycles of denaturation at 94ºC for 30 sec, annealing at 62ºC (for p53), 60ºC (for Rb) or 67ºC (for β-Actin) for 30 sec and extension at 72ºC for 50 sec. Primer sequences used are shown in **Table 1S.**

**Western Blot**

Western blotting analysis of whole cell extracts of exponentially growing cells was performed as previously described (11) using as primary antibodies anti-p53 (1:500 dilution; Santa Cruz Biotechnology, Santa Cruz, CA), anti-Rb (1:750 dilution; BD-Pharmingen) and anti-β-Actin (1:20.000; Sigma).

**MSC differentiation**

For differentiation assays (11, 35), ASCs and BM-MSCs were plated at $2x10^4$ cells/$cm^2$ in MesenCult medium and were allowed to adhere for 24 hours. Culture medium was then replaced with specific differentiation inductive media. For adipogenic differentiation, cells were cultured in AdipoCult Differentiation Kit (Stem Cell Technologies) for 15 to 20 days. Differentiated cell cultures were stained with Oil Red O (Amresco, Solon, OH). For osteogenic differentiation, cells were cultured in Osteogenic MSCs Differentiation BulletKit (Lonza) for 2, 5, 10 or 16 days. Total or partially differentiated ASC and BM-MSC cultures were either infected with Ad-CMV-Cre or checked for the degree of differentiation by Q-RT-PCR analysis of osteogenic markers and by Alizarin Red S (Sigma) staining.

**Flow Cytometry**

The immunophenotype of cultured MSCs was analyzed by flow cytometry as previously described (13) using fluorochrome-conjugated monoclonal antibodies for Sca-1, CD11b, CD34, CD45, CD44, and CD29 (Becton Dickinson).

**Quantitative PCR**

Total RNA was extracted from MSC cultures induced to differentiate towards osteogenic lineage. First-strand cDNA synthesis was performed using the First-Strand cDNA Synthesis Kit

(Amersham) and the expression of the osteogenic-specific differentiation markers collagen type I, osteopontin, osteocalcin, osterix and BMP-4 was assessed by Q-RT-PCR using SYBR Green PCR Kit (Qiagen) (36). β-actin was used as a housekeeping gene. The following PCR conditions were used: 5 min at 94ºC, 35 cycles of 30 seconds at 94ºC followed by 50 seconds at 60ºC and 50 seconds at 72ºC and a final extension of 10 min at 72ºC. Up-regulation of the expression of osteogenic markers as compared to undifferentiated MSC cultures was statistically analyzed using the Student's t-test. Primer sequences used are shown in **Table 1S.**

***In vivo* tumorigenic assay**

NOD/SCID IL2Rγ$^{-/-}$ (NSG) mice were obtained from The Jackson Laboratory. All mice were housed under specific pathogen-free conditions, fed ad libitum according to animal facilities guidelines, and used at 8 to 12 weeks old (37). NSG mice were inoculated subcutaneously with $5\times10^6$ mutant undifferentiated ASCs/BM-MSCs, $5\times10^6$ p53$^{-/-}$Rb$^{-/-}$ ASC/BM-MSC-derived osteogenic progenitors or $2\times10^5$ primary tumor-derived cells, according to the United Kingdom Coordinating Committee for Cancer Research guidelines for the welfare of animals in experimental cancer research. Animals were killed when tumors reached 1 cm$^3$ or 150 days after infusion. Latency and tumor incidence were represented using Kaplan-Meier curves. The log-rank test and the hazard ratio with the 95% confidence interval were used to estimate significant differences among groups (38, 39). Upon tumor removal, half the tumor was mechanically disaggregated to establish *ex vivo* MSC-transformed cell lines as previously described (11). The remaining portion of the tumor was used for immunohistopathology analysis (40).

**Gene expression Profiling (GEP)**

Primary (wt, p53$^{-/-}$, Rb$^{-/-}$p53$^{-/-}$ and Rbp53-10Days) as well as tumoral (Tp53, TRbp53 and TRbp53-10Days) ASC and BM-MSCs were collected during the exponential cell growth and

stabilized in RNA later (Ambion, Austin, TX) solution until RNA extraction. RNA was isolated using the Agilent Total RNA Isolation Kit (Agilent Technologies, Palo Alto, CA) and its quality checked in the Agilent 2100 Bioanalyzer. Total RNA samples were labeled with Cy3 using the Quick-Amp Labeling kit and hybridized with the Whole Mouse Genome Microarray (G4122F), following Manufacturer's instructions (Agilent Technologies, CA). Each sample was labeled and hybridized as independent triplicates (41). Primary data was examined using GeneSpring 11.0 software (Silicon Genetics, Redwood City, CA). Gene expression in the control and experimental groups was compared. Only genes satisfying the threshold of *P* value < 0.05 and a fold change expression> 2 were included and assigned as significant. Analysis of pathways significantly altered in the experimental groups was performed using the Ingenuity Pathway software 8.0 (IPA; Ingenuity Systems, Inc., Redwood City, CA). Microarray data has been deposited and is available at Gene Expression Omnibus (http://www.ncbi.nlm.nih.gov/geo/).

**Immunohistopathology analysis**

Tumor samples were fixed in formol, embedded in paraffin, cut into 4-µm sections, and stained with haematoxylin and eosin (H&E) and a panel of specific primary antibodies (all from Upstate/Millipore) against: Caldesmon (1:500 dilution), Smooth-muscle Actin (1:50 dilution) and myosin (1:100 dilution). The secondary HRP-conjugated rabbit anti-IgG antibody was used at 1:100 dilution for 30 min. The immunostaining was visualized using diaminobenzidine and counterstained with hematoxylin. All the washing steps were done in PBS (42). The degree of osteogenic differentiation in the tumors was quantified by analyzing 20 images (10x magnification) randomly taken from 3 different tumors of each experimental condition. The area of osteoid matrix was quantified as the percentage of "osteoid matrix/total area" using the Image J software (NIH, Bethesda, MD). The mean and standard deviation of the percentage of osteoid area in each condition was calculated.

## CONFLICT OF INTEREST

The authors have no conflict of interest to disclose.

## ACKNOWLEDGMENTS

We thank the Andalusian Platform of Bioinformatics (PAB; University of Málaga) for providing access to IPA software. This work was supported by the Instituto de Salud Carlos III/FEDER (PI10/00449 to P.M and CP11/00024 -Miguet Servet Program- to R.Ro); the Junta de Andalucía/FEDER (P08-CTS-3678 to P.M), the MINECO (Fondo Especial del Estado para Dinamización de la Economía y Empleo PLE-2009-0111 to P.M and SAF2010-15106 to M.L.T), The Spanish Association Against Cancer (Junta Provincial de Albacete-CI110023 to P.M and Junta Provincial de Granada to R.Ro), and Health Canada (H4084-112281 to P.M, R.Ro and M.R-M). R.Ru was supported by a fellowship of the ISCIII/FEDER.

## REFERENCES


1. Garcia-Castro J, Trigueros C, Madrenas J, Perez-Simon JA, Rodriguez R, Menendez P. Mesenchymal stem cells and their use as cell replacement therapy and disease modelling tool. *J Cell Mol Med* 2008; **12**: 2552-2565.

2. Rodriguez R, Garcia-Castro J, Trigueros C, Garcia Arranz M, Menendez P. Multipotent mesenchymal stromal cells: clinical applications and cancer modeling. *Adv Exp Med Biol* 2012; **741**: 187-205.

3. Rodriguez R, Rubio R, Menendez P. Modeling sarcomagenesis using multipotent mesenchymal stem cells. *Cell Res* 2012; **22**: 62-67.

4. Helman LJ, Meltzer P. Mechanisms of sarcoma development. *Nat Rev Cancer* 2003; **3**: 685-694.

5. Malkin D, Li FP, Strong LC, Fraumeni JF, Jr., Nelson CE, Kim DH *et al.* Germ line p53 mutations in a familial syndrome of breast cancer, sarcomas, and other neoplasms. *Science* 1990; **250**: 1233-1238.

6. Li H, Fan X, Kovi RC, Jo Y, Moquin B, Konz R *et al.* Spontaneous expression of embryonic factors and p53 point mutations in aged mesenchymal stem cells: a model of age-related tumorigenesis in mice. *Cancer Res* 2007; **67**: 10889-10898.

7. Miura M, Miura Y, Padilla-Nash HM, Molinolo AA, Fu B, Patel V *et al.* Accumulated chromosomal instability in murine bone marrow mesenchymal stem cells leads to malignant transformation. *Stem Cells* 2006; **24**: 1095-1103.

8. Mohseny AB, Szuhai K, Romeo S, Buddingh EP, Briaire-de Bruijn I, de Jong D *et al.* Osteosarcoma originates from mesenchymal stem cells in consequence of aneuploidization and genomic loss of Cdkn2. *J Pathol* 2009; **219**: 294-305.

9. Tolar J, Nauta AJ, Osborn MJ, Panoskaltsis Mortari A, McElmurry RT, Bell S *et al.* Sarcoma derived from cultured mesenchymal stem cells. *Stem Cells* 2007; **25**: 371-379.

10. Armesilla-Diaz A, Elvira G, Silva A. p53 regulates the proliferation, differentiation and spontaneous transformation of mesenchymal stem cells. *Exp Cell Res* 2009; **315**: 3598-3610.

11. Rodriguez R, Rubio R, Gutierrez-Aranda I, Melen GJ, Elosua C, Garcia-Castro J *et al.* FUS-CHOP fusion protein expression coupled to p53 deficiency induces liposarcoma in mouse but not in human adipose-derived mesenchymal stem/stromal cells. *Stem Cells* 2011; **29**: 179-192.

12. Rodriguez R, Rubio R, Masip M, Catalina P, Nieto A, de la Cueva T *et al.* Loss of p53 induces tumorigenesis in p21-deficient mesenchymal stem cells. *Neoplasia* 2009; **11**: 397-407.

13. Rubio R, Garcia-Castro J, Gutierrez-Aranda I, Paramio J, Santos M, Catalina P *et al.* Deficiency in p53 but not retinoblastoma induces the transformation of mesenchymal stem cells in vitro and initiates leiomyosarcoma in vivo. *Cancer Res* 2010; **70**: 4185-4194.

14. Lengner CJ, Steinman HA, Gagnon J, Smith TW, Henderson JE, Kream BE *et al.* Osteoblast differentiation and skeletal development are regulated by Mdm2-p53 signaling. *J Cell Biol* 2006; **172**: 909-921.

15. Tataria M, Quarto N, Longaker MT, Sylvester KG. Absence of the p53 tumor suppressor gene promotes osteogenesis in mesenchymal stem cells. *J Pediatr Surg* 2006; **41**: 624-632; discussion 624-632.

16. Molchadsky A, Shats I, Goldfinger N, Pevsner-Fischer M, Olson M, Rinon A *et al.* p53 plays a role in mesenchymal differentiation programs, in a cell fate dependent manner. *PLoS One* 2008; **3**: e3707.

17. Calo E, Quintero-Estades JA, Danielian PS, Nedelcu S, Berman SD, Lees JA. Rb regulates fate choice and lineage commitment in vivo. *Nature* 2010; **466**: 1110-1114.

18. De Falco G, Comes F, Simone C. pRb: master of differentiation. Coupling irreversible cell cycle withdrawal with induction of muscle-specific transcription. *Oncogene* 2006; **25**: 5244-5249.

19. Gutierrez GM, Kong E, Sabbagh Y, Brown NE, Lee JS, Demay MB *et al.* Impaired bone development and increased mesenchymal progenitor cells in calvaria of RB1-/- mice. *Proc Natl Acad Sci U S A* 2008; **105**: 18402-18407.

20. Thomas DM, Carty SA, Piscopo DM, Lee JS, Wang WF, Forrester WC *et al.* The retinoblastoma protein acts as a transcriptional coactivator required for osteogenic differentiation. *Mol Cell* 2001; **8**: 303-316.

21. Berman SD, Calo E, Landman AS, Danielian PS, Miller ES, West JC *et al.* Metastatic osteosarcoma induced by inactivation of Rb and p53 in the osteoblast lineage. *Proc Natl Acad Sci U S A* 2008; **105**: 11851-11856.

22. Walkley CR, Qudsi R, Sankaran VG, Perry JA, Gostissa M, Roth SI *et al.* Conditional mouse osteosarcoma, dependent on p53 loss and potentiated by loss of Rb, mimics the human disease. *Genes Dev* 2008; **22**: 1662-1676.

23. Lin PP, Pandey MK, Jin F, Raymond AK, Akiyama H, Lozano G. Targeted mutation of p53 and Rb in mesenchymal cells of the limb bud produces sarcomas in mice. *Carcinogenesis* 2009; **30**: 1789-1795.

24. Tang N, Song WX, Luo J, Haydon RC, He TC. Osteosarcoma development and stem cell differentiation. *Clin Orthop Relat Res* 2008; **466**: 2114-2130.

25. Danielson LS, Menendez S, Attolini CS, Guijarro MV, Bisogna M, Wei J *et al.* A differentiation-based microRNA signature identifies leiomyosarcoma as a mesenchymal stem cell-related malignancy. *Am J Pathol* 2010; **177**: 908-917.

26. Choi J, Curtis SJ, Roy DM, Flesken-Nikitin A, Nikitin AY. Local mesenchymal stem/progenitor cells are a preferential target for initiation of adult soft tissue sarcomas associated with p53 and Rb deficiency. *Am J Pathol* 2010; **177**: 2645-2658.

27. Kirsch DG, Dinulescu DM, Miller JB, Grimm J, Santiago PM, Young NP *et al.* A spatially and temporally restricted mouse model of soft tissue sarcoma. *Nat Med* 2007; **13**: 992-997.

28. Clark-Knowles KV, Senterman MK, Collins O, Vanderhyden BC. Conditional inactivation of Brca1, p53 and Rb in mouse ovaries results in the development of leiomyosarcomas. *PLoS One* 2009; **4**: e8534.

29. Hernando E, Charytonowicz E, Dudas ME, Menendez S, Matushansky I, Mills J *et al.* The AKT-mTOR pathway plays a critical role in the development of leiomyosarcomas. *Nat Med* 2007; **13**: 748-753.

30. Shimizu T, Ishikawa T, Sugihara E, Kuninaka S, Miyamoto T, Mabuchi Y *et al.* c-MYC overexpression with loss of Ink4a/Arf transforms bone marrow stromal cells into osteosarcoma accompanied by loss of adipogenesis. *Oncogene* 2010; **29**: 5687-5699.

31. Benassi MS, Molendini L, Gamberi G, Magagnoli G, Ragazzini P, Gobbi GA *et al.* Involvement of INK4A gene products in the pathogenesis and development of human osteosarcoma. *Cancer* 2001; **92**: 3062-3067.

32. Lopez-Guerrero JA, Lopez-Gines C, Pellin A, Carda C, Llombart-Bosch A. Deregulation of the G1 to S-phase cell cycle checkpoint is involved in the pathogenesis of human osteosarcoma. *Diagn Mol Pathol* 2004; **13**: 81-91.

33. Bianco P, Robey PG, Simmons PJ. Mesenchymal stem cells: revisiting history, concepts, and assays. *Cell Stem Cell* 2008; **2**: 313-319.

34. Martinez-Cruz AB, Santos M, Lara MF, Segrelles C, Ruiz S, Moral M *et al.* Spontaneous squamous cell carcinoma induced by the somatic inactivation of retinoblastoma and Trp53 tumor suppressors. *Cancer Res* 2008; **68**: 683-692.

35. Sanchez L, Gutierrez-Aranda I, Ligero G, Rubio R, Munoz-Lopez M, Garcia-Perez JL *et al.* Enrichment of human ESC-derived multipotent mesenchymal stem cells with immunosuppressive and anti-inflammatory properties capable to protect against experimental inflammatory bowel disease. *Stem Cells* 2011; **29**: 251-262.

36. Menendez P, Catalina P, Rodriguez R, Melen GJ, Bueno C, Arriero M *et al.* Bone marrow mesenchymal stem cells from infants with MLL-AF4+ acute leukemia harbor and express the MLL-AF4 fusion gene. *J Exp Med* 2009; **206**: 3131-3141.

37. Bueno C, Montes R, de la Cueva T, Gutierrez-Aranda I, Menendez P. Intra-bone marrow transplantation of human CD34(+) cells into NOD/LtSz-scid IL-2rgamma(null) mice permits multilineage engraftment without previous irradiation. *Cytotherapy* 2010; **12**: 45-49.

38. Chillon MC, Gomez-Casares M, Lopez-Jorge CE, Rodriguez-Medina C, Molines A, Sarasquete ME *et al.* Prognostic significance of FLT3 mutational status and expression levels in MLL-AF4 and MLL-germline Acute Lymphoblastic Leukemia. *Leukemia* 2012: (in press).

39. Menendez P, Perez-Simon JA, Mateos MV, Caballero MD, Gonzalez M, San-Miguel JF *et al.* Influence of the different CD34+ and CD34- cell subsets infused on clinical outcome after non-myeloablative allogeneic peripheral blood transplantation from human leucocyte antigen-identical sibling donors. *Br J Haematol* 2002; **119**: 135-143.

40. Gutierrez-Aranda I, Ramos-Mejia V, Bueno C, Munoz-Lopez M, Real PJ, Macia A *et al.* Human induced pluripotent stem cells develop teratoma more efficiently and faster than human embryonic stem cells regardless the site of injection. *Stem Cells* 2010; **28**: 1568-1570.

41. Shojaei F, Menendez P. Molecular profiling of candidate human hematopoietic stem cells derived from human embryonic stem cells. *Exp Hematol* 2008; **36**: 1436-1448.

42. Barroso-delJesus A, Lucena-Aguilar G, Sanchez L, Ligero G, Gutierrez-Aranda I, Menendez P. The Nodal inhibitor Lefty is negatively modulated by the microRNA miR-302 in human embryonic stem cells. *FASEB J* 2011; **25**: 1497-1508.

**Table 1. In vivo tumor formation ability of Wt, $p53^{-/-}$, $Rb^{-/-}$, $Rb^{-/-}p53^{-/-}$ BM-MSCs inoculated into immunodeficient mice**

| BM-MSC genotype | Tumour incidence | Latency | Histological analysis |
|---|---|---|---|
| Wt | 0/8 | NT | - |
| $Rb^{-/-}$ | 0/9 | NT | - |
| $p53^{-/-}$ | 6/12* | 65-148 (107)[2] | Leiomyosarcoma |
| $Rb^{-/-}$ $p53^{-/-}$ | 19/25* | 31-109 (65)[2] | Leiomyosarcoma |

*. Chi-square p-value<0.05 versus Wt or $Rb^{-/-}$ values.
NT. No tumour was detected after 150 days.
[2]. Range of days for tumour development (mean)

**Table 2. In vivo tumor formation ability of $Rb^{-/-}p53^{-/-}$ BM-MSC/ASC osteogenic derivatives**

| | Tumour incidence | Latency | Histological analysis |
|---|---|---|---|
| BM-Rbp53-Undiff | 19/25 | 31-109 (65)[1] | Leiomyosarcoma |
| BM-Rbp53-2Days | 11/15 | 35-100 (63)[1] | Osteosarcoma |
| BM-Rbp53-5Days | 12/15 | 22-107 (62)[1] | Osteosarcoma |
| BM-Rbp53-10Days | 14/20 | 38-97 (68)[1] | Osteosarcoma |
| ASC-Rbp53-Undiff | 3/5 | 51-58 (56)[1] | Leiomyosarcoma |
| ASC-Rbp53-2Days | 0/5 | NT | - |
| ASC-Rbp53-5Days | 0/5 | NT | - |
| ASC-Rbp53-10Days | 0/5 | NT | - |

[1]. Range of days for tumour development (mean)

NT, No tumour was detected after 150 days.

## LEGENDS TO FIGURES

**Figure 1. *p53*$^{-/-}$ and *Rb*$^{-/-}$*p53*$^{-/-}$ deficient undifferentiated BM-MSCs give rise to leiomyiosarcoma *in vivo*.** **(A)** Cartoon representing how wt, Rb$^{loxP/loxP}$, p53$^{loxP/loxP}$ and Rb$^{loxP/loxP}$p53$^{loxP/loxP}$ MSCs were harvested from adipose tissue (ASCs) and bone marrow (BM-MSCs) and infected with Cre-expressing adenoviral vectors (Adeno-Cre) generating wt, Rb$^{-/-}$, p53$^{-/-}$ and Rb$^{-/-}$p53$^{-/-}$ ASC/BM-MSCs. **(B)** Genomic PCR confirming depletion of either p53 or Rb in the indicated MSC genotypes. β-Actin was used as a housekeeping control. **(C)** Western blot performed in the presence or absence of camptothecin (CPT;0.5 μmol/L for 24 hours) confirming lack of expression of either p53 or Rb protein in the indicated MSC genotypes. β-Actin was used as a loading control. **(D)** Tumor formation curves for distinct BM-MSC genotypes. The estimated tumor incidence between p53$^{-/-}$ and Rbp53$^{-/-}$ after 120 days was 28% *vs* 75%, respectively (p=0.04). **(E)** Histological analysis of tumors developed in NOD/SCID mice infused with p53$^{-/-}$ and Rb$^{-/-}$p53$^{-/-}$ BM-MSCs. Staining is shown for H&E, caldesmon, smooth muscle actin and myosin. Original magnification is 20x. Insets show 60x magnification.

**Figure 2. Comparative analysis of the gene expression profiling between p53$^{-/-}$, Rb$^{-/-}$p53$^{-/-}$, Tp53 and TRbp53 cells supports the leiomyosarcoma histological diagnosis regardless the source of the MSCs (fat or BM). (A)** After gene expression microarray analysis, the genes differentially expressed (p value<0.05; expression >2-fold up or down) in p53$^{-/-}$ and Rb$^{-/-}$p53$^{-/-}$ ASCs/BM-MSCs and their derived tumors Tp53 and TRbp53 were compared to wt-ASC/BM-MSC and analyzed using the IPA software. IPA software-based data mining selected those genes differentially expressed and classified as associated to sarcomas. As it can be observed, all the genes differentially expressed were associated to leiomyosarcoma or other forms of muscle-derived sarcoma rather than sarcomas affecting other tissues, further confirming molecularly the leiomyosarcoma diagnosis regardless the source of the MSCs. **(B)** Venn diagrams representing

the number of genes differentially expressed between Tp53 (left) and TRbp53 (right) tumor-derived cells and wt ASC or wt BM-MSCs. As many as 40-62% of the differentially expressed genes between tumoral MSCs and wt MSCs were common for ASCs and BM-MSCs, further confirming that the tissue source of MSC does not seem crucial in determining the phenotype of sarcoma development *in vivo*. **(C)** Scheme provided by IPA software specifically showing genes related to leiomyosarcoma development commonly or uniquely altered in Tp53 and TRbp53 as compared to wt MSCs (light/dark grey color correspond to down/upregulated gene expression). NF-kB, PTEN, PI3K/AKT and IL-8 signaling pathways are the most commonly altered routes in both Tp53 and TRbp53.

**Figure 3. Osteogenic differentiation of $Rb^{loxP/loxP}p53^{loxP/loxP}$ BM-MSCs/ASCs and subsequent Adeno-Cre infection. (A)** Scheme of the osteogenic differentiation protocol with Adeno-Cre infection after 2, 5 and 10 days to generate mutant $Rb^{-/-}p53^{-/-}$ BM-MSCs/ASCs osteogenic progenitors. **(B)** Genomic PCR confirming almost complete depletion of both p53 and Rb in $Rb^{loxP/loxP}p53^{loxP/loxP}$ BM-MSCs (left) and $Rb^{loxP/loxP}p53^{loxP/loxP}$ ASCs (right) after Adeno-Cre infection. **(C)** Q-RT-PCR confirming the up-regulation of the indicated osteogenic markers upon induced osteogenic differentiation (*,p-value<0.05 *vs* undifferentiated cells). **(D)** Alizarin Red staining confirming functional *in vitro* osteogenic differentiation over time.

**Figure 4. Osteogenic-committed $Rb^{-/-}p53^{-/-}$ BM-MSCs originate osteosarcoma *in vivo*. (A)** Tumor formation curves for BM-Rbp53-Undiff, -2Days, -5Days or -10Days cells. **(B)** H&E staining (10x [top panels] and 40x [bottom panels]) of tumors developed from undifferentiated $Rb^{-/-}p53^{-/-}$ BM-MSCs (left) or osteogenic-committed $Rb^{-/-}p53^{-/-}$ BM-MSCs (middle and right panels). Os: osteoid matrix. **(C)** The osteoid areas of 20 images randomly taken from 3 different tumors were quantified using the Image J software. The mean and standard deviation of the percentages of

osteoid area for each condition (bottom panel) and an example of quantification (top panel) are represented. Numbers in the top panel indicate the proportion of each individual osteoid area relative to the entire area analyzed. The areas of image without tissue were not computed (ex). **(D)** Q-RT-PCR analysis of an early (oxterix) and a late (osteocalcin) osteogenic marker in TBMRbp53-Undiff, -2Days, -5Days and -10Days tumor cell lines. **(B-D)** These data indicate that the depletion of Rb and p53 in more differentiated cells originates the formation of more differentiated osteosarcomas.

**Figure 5. Gene expression profiling supports the osteosarcoma histological diagnosis of TBM-Rbp53-10Days tumors and reveals significant differences between BM- and ASC-Rbp53-10Days cells. (A) G**enes differentially expressed (p value<0.05; expression >2-fold up or down) in ASC-Rbp53-10Days, BM-Rbp53-10Days and TBM-Rbp53-10Days cells as compared to wt-ASC/BM-MSC were analyzed using the IPA software. IPA-based data mining selected those genes differentially expressed and classified as associated to sarcomas. While ASC-Rbp53-10Days are related to muscle-derived sarcomas despite the osteogenic priming TBM-Rbp53-10Days tumor cells are associated to osteosarcoma. **(B)** Venn diagrams representing the number of genes differentially expressed between ASC-Rbp53-10Days or BM-Rbp53-10Days and wt ASC or wt BM-MSCs. After the osteogenic priming of the $Rb^{-/-}p53^{-/-}$ ASCs and BM-MSCs, the percentage of overlapping genes was ~28%, much lower than tumors developed from the corresponding undifferentiated cells (~40-60%, Fig 2B). **(C)** List of the most significantly modulated pathways and upstream regulators signaling generated with the genes specifically altered in ASC-Rbp53-10Days cells (left column) and BM-Rbp53-10Days cells (right column).

**LEGENDS TO SUPPLEMENTARY FIGURES**

**Supplementary Figure S1. Phenotypic and functional characterization of the MSC genotypes used in the present study. (A)** Immunophenotypic profile of the indicated BM-MSC genotypes analyzed by flow cytometry. Representative dot plots are shown for Sca-1, CD29, CD44, CD14, CD11b, and CD45. Empty lines represent the irrelevant isotypes. Red-filled lines display antibody-specific staining. **(B)** Adipogenic (Oil red staining; top panels) and osteogenic (Alizarin red staining; bottom panels) differentiation potential of BM-MSCs with the distinct genotypes indicated. Original magnification is indicated.

**Supplementary Figure S2. Histological analysis of tumors developed in NOD/SCID mice inoculated with $p53^{-/-}$ (left) and $Rb^{-/-}p53^{-/-}$ (right) ASCs**. Staining is shown for H&E, caldesmon, smooth muscle actin and myosin. Insets show 40x magnification.

**Supplementary Figure S3. Immortalized $p53^{-/-}$ and $Rb^{-/-}p53^{-/-}$ cell lines *ex vivo*-derived from primary tumors reinitiate sarcoma development upon secondary inoculation in NOD/SCID with 100% penetrance and much shorter latency. (A)** Tumoral cell lines *ex vivo*-derived from primary leiomyosarcomas formed by $p53^{-/-}$ and $Rb^{-/-}p53^{-/-}$ BM-MSCs (termed Tbmp53 and TbmRbp53, respectively) retained p53 and/or Rb depletion. **(B)** *In vivo* tumor formation ability (penetrance and latency) of TBM-p53-1 and TBM-Rbp53-1 cell lines inoculated in secondary immunodeficient mice. **(C)** Representative histological analysis of secondary tumors developed in NOD/SCID mice infused with TBM-p53 and TBM-Rbp53. Staining is shown for H&E, caldesmon and smooth muscle actin. Original magnification is 20x.

**Supplementary Figure S4.** Complete list of genes associated to sarcoma differentially expressed (p value<0.05; expression >2-fold up or down) in $p53^{-/-}$ and $Rb^{-/-}p53^{-/-}$ ASC/BM-MSC and their derived tumors Tp53 and TRbp53 as compared to wt-ASC/BM-MSC (see Figure 2A).

**Figure S5. Immortalized $Rb^{-/-}p53^{-/-}$ cell lines *ex vivo*-derived from primary tumors reproduce osteosarcoma development upon secondary inoculation in NOD/SCID with 100% penetrance and much shorter latency. (A)** Tumoral cell lines *ex vivo*-derived from primary sarcomas formed by either $Rb^{-/-}p53^{-/-}$ undifferentiated BM-MSCs (TBM-Rbp53-Undiff) or $Rb^{-/-}p53^{-/-}$ BM-MSC-derived osteogenic progenitors (TBM-Rbp53-2Days and TBM-Rbp53-10Days) retained p53 and Rb depletion. **(B)** Tumor incidence, latency and histological analysis (H&E staining, 10x original magnification; Os: osteoid matrix) of secondary tumors developed in NOD/SCID mice inoculated with TBM-Rbp53-Undiff (top), TBM-Rbp53-2Days (middle) and TBM-Rbp53-10Days (bottom) cell lines.

**Supplementary Figure S6.** Complete list of genes associated to sarcoma differentially expressed (p value<0.05; expression >2-fold up or down) in ASC-Rbp53-10Days, BM-Rbp53-10Days and TBM-Rbp53-10Days cells as compared to wt-ASC/BM-MSC (see Figure 5A).

**Table 1. In vivo tumor formation ability of Wt, $p53^{-/-}$, $Rb^{-/-}$, $Rb^{-/-}p53^{-/-}$ BM-MSCs inoculated into immunodeficient mice**

| BM-MSC genotype | Tumour incidence | Latency | Histological analysis |
|---|---|---|---|
| Wt | 0/8 | NT | - |
| $Rb^{-/-}$ | 0/9 | NT | - |
| $p53^{-/-}$ | 6/12* | 65-148 (107)[2] | Leiomyosarcoma |
| $Rb^{-/-}$ $p53^{-/-}$ | 19/25* | 31-109 (65)[2] | Leiomyosarcoma |

*. Chi-square p-value<0.05 versus Wt or $Rb^{-/-}$ values.

NT. No tumour was detected after 150 days.

2. Range of days for tumour development (mean)

**Table 2. In vivo tumor formation ability of $Rb^{-/-}p53^{-/-}$ BM-MSC/ASC osteogenic derivatives**

| | Tumour incidence | Latency | Histological analysis |
|---|---|---|---|
| BM-Rbp53-Undiff | 19/25 | 31-109 (65)[1] | Leiomyosarcoma |
| BM-Rbp53-2Days | 11/15 | 35-100 (63)[1] | Osteosarcoma |
| BM-Rbp53-5Days | 12/15 | 22-107 (62)[1] | Osteosarcoma |
| BM-Rbp53-10Days | 14/20 | 38-97 (68)[1] | Osteosarcoma |
| ASC-Rbp53-Undiff | 3/5 | 51-58 (56)[1] | Leiomyosarcoma |
| ASC-Rbp53-2Days | 0/5 | NT | - |
| ASC-Rbp53-5Days | 0/5 | NT | - |
| ASC-Rbp53-10Days | 0/5 | NT | - |

1. Range of days for tumour development (mean)

NT, No tumour was detected after 120 days.

Rubio et al. Figure 1

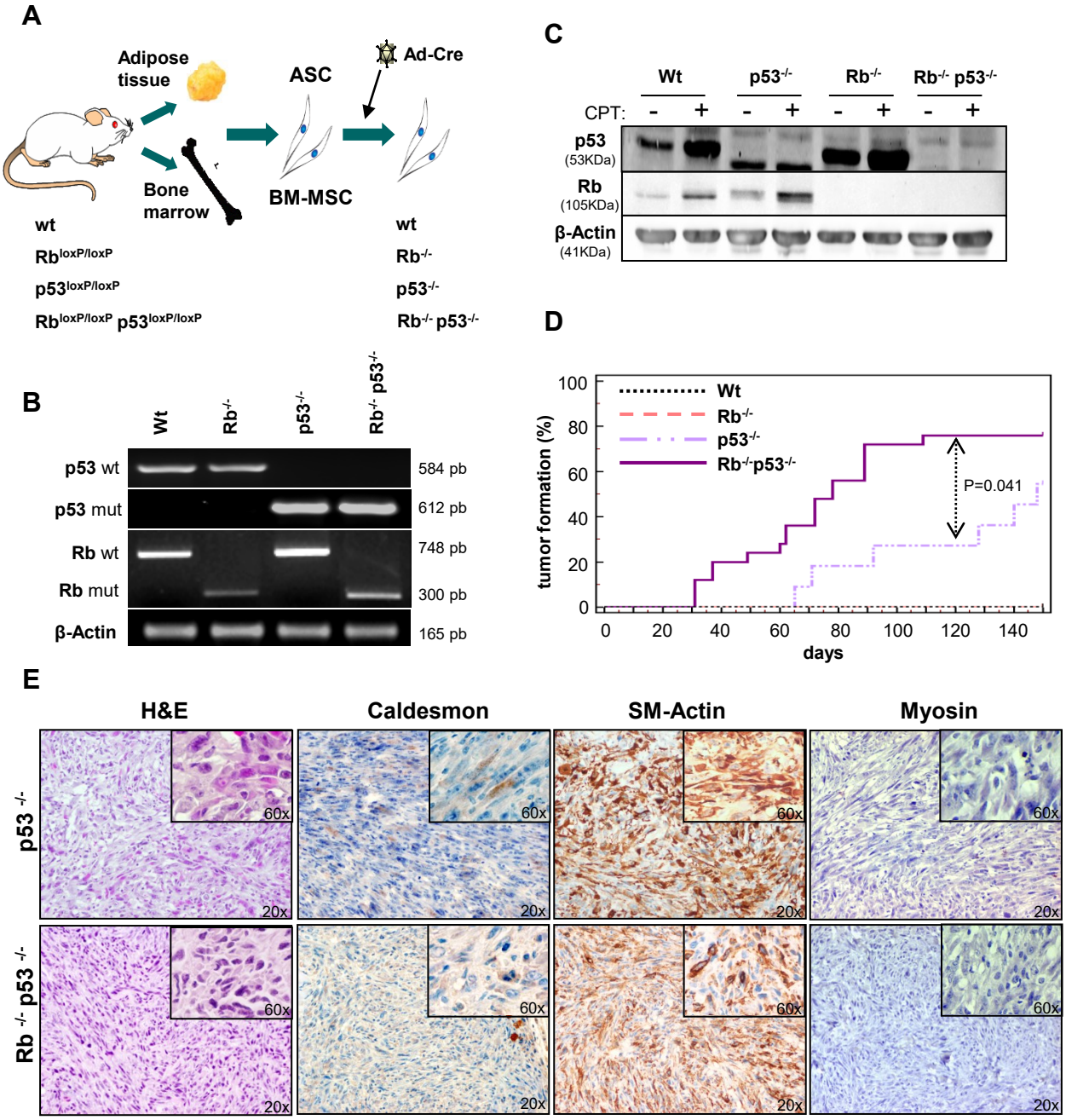

Rubio et al. Figure 2

**A**

| | | Sarcoma categories | p-Value | Molecules |
|---|---|---|---|---|
| p53 vs wt | ASC | myosarcoma | 4.68E-04 | 19 |
| | | sarcoma | 6,15E-04 | 29 |
| | | rhabdomyosarcoma | 1.01E-03 | 18 |
| | | Tumorig.of muscle | 1,58E-03 | 7 |
| | BM | Tumorig.of muscle | 2,95E-04 | 8 |
| | | hyperplasia of muscle | 9.98E-04 | 7 |
| | | Develop. of sarcoma | 7,87E-03 | 6 |
| Rbp53 vs wt | ASC | sarcoma | 4.44E-06 | 101 |
| | | leiomyomatosis | 2,90E-05 | 98 |
| | BM | myosarcoma | 2.70E-10 | 41 |
| | | sarcoma | 2,61E-09 | 78 |
| | | soft tissue sarcoma | 7,60E-09 | 51 |
| | | rhabdomyosarcoma | 1,76E-08 | 31 |
| Tp53 vs wt | ASC | leiomyomatosis | 4,39E-07 | 134 |
| | | myosarcoma | 1.44E-04 | 53 |
| | | leiomyosarcoma | 4,21E-04 | 22 |
| | BM | myosarcoma | 1.15E-04 | 40 |
| | | sarcoma | 3.17E-04 | 87 |
| | | leiomyosarcoma | 5,86E-04 | 17 |
| TRbp53 vs wt | ASC | leiomyomatosis | 6,22E-07 | 113 |
| | | sarcoma | 5.15E-05 | 105 |
| | | myosarcoma | 1,88E-04 | 45 |
| | BM | soft tissue sarco ma | 1,63E-04 | 86 |
| | | leiomyomatosis | 2,13E-04 | 142 |

**B**

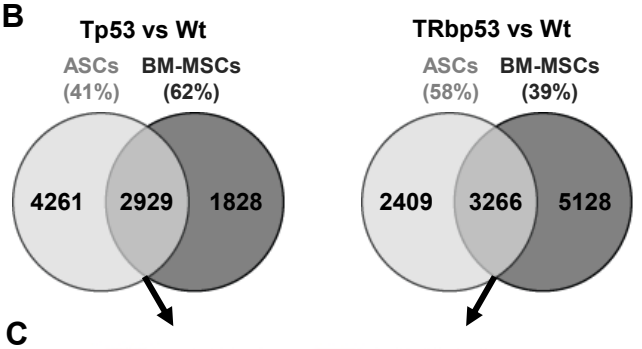


**C**

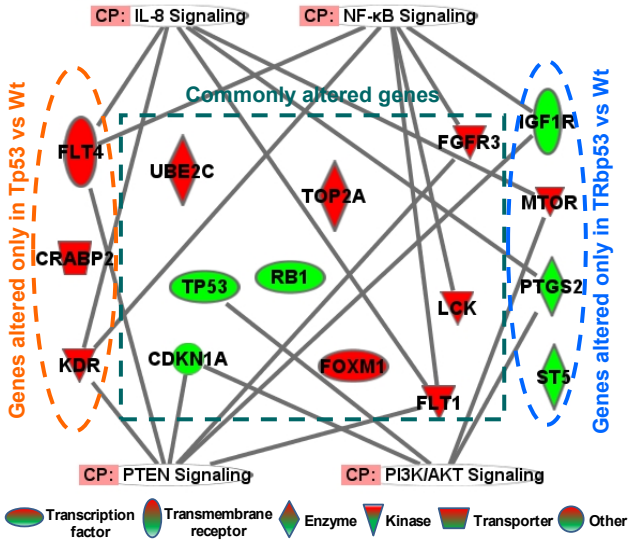

Rubio et al. Figure 3

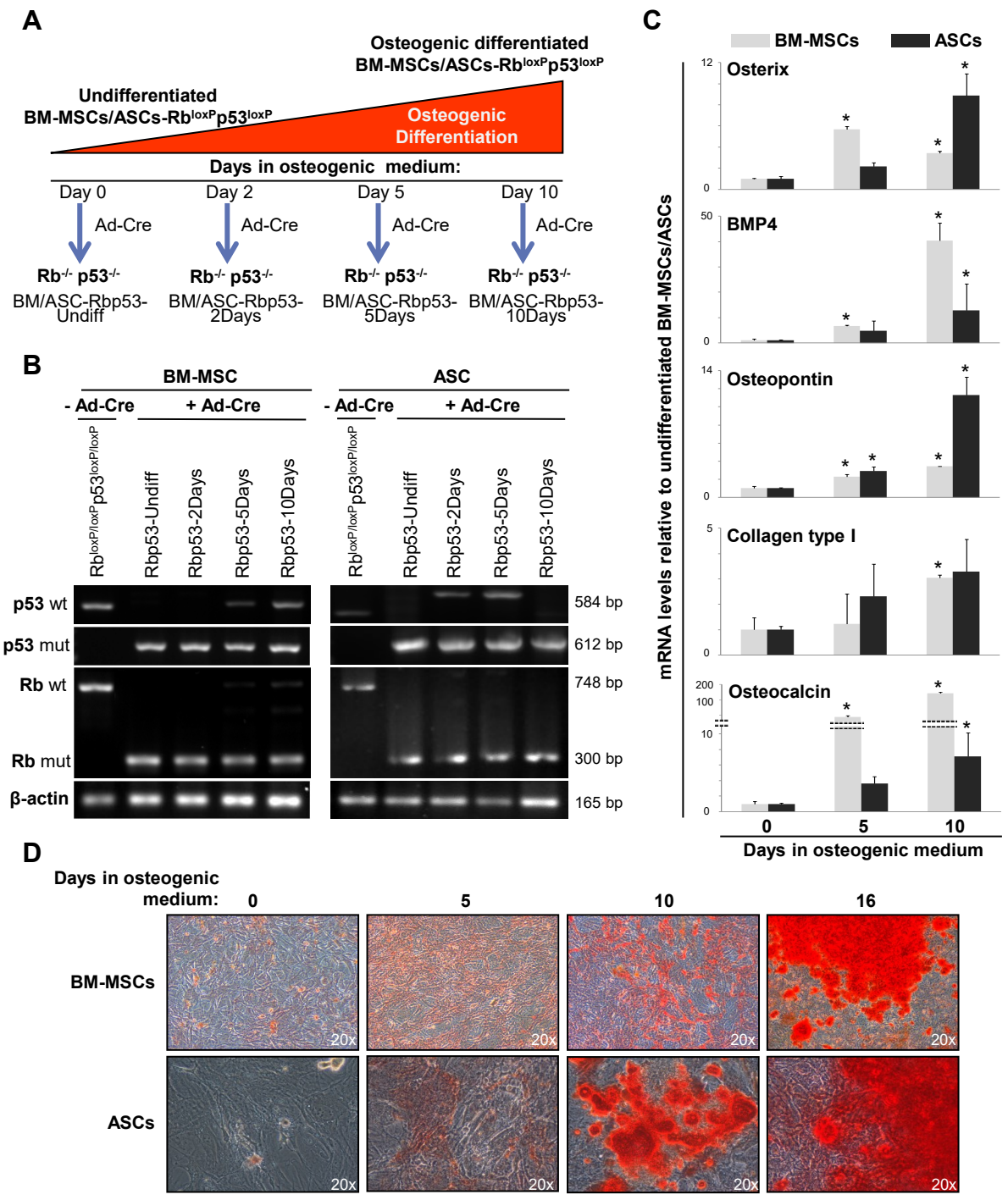

Rubio et al. Figure 4

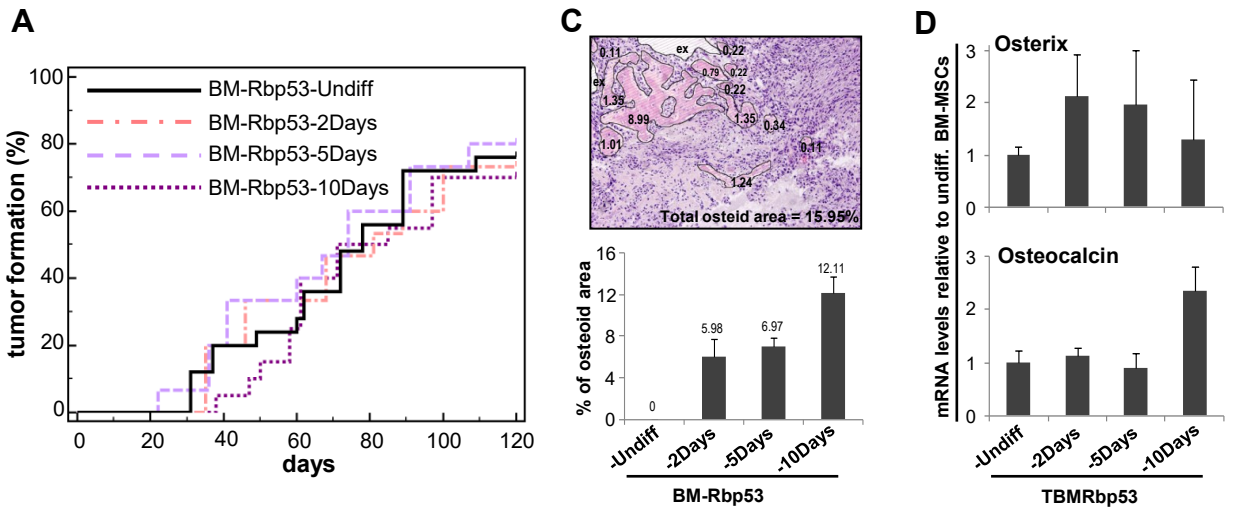


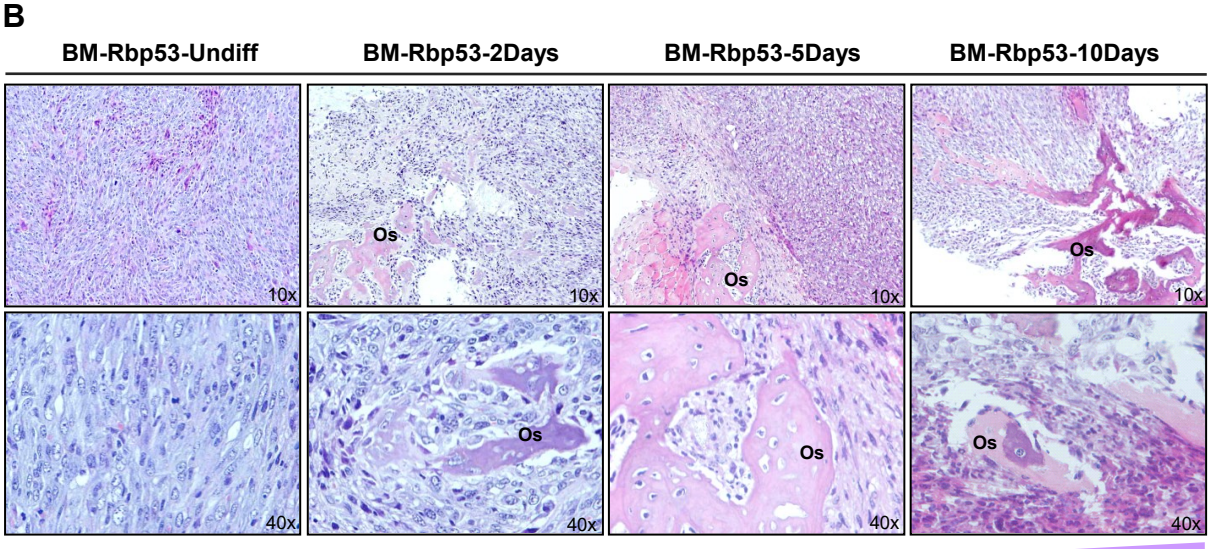


LEIOMYOSARCOMA

**OSTEOSARCOMA** (degree of differentiation)

**Rubio et al. Figure 5**

**A**

| | | Sarcoma categories | p-Value | Molecules |
|---|---|---|---|---|
| **Rbp53-10Days vs wt** | ASC | myosarcoma | 1,64E-08 | 31 |
| | | leiomyosarcoma | 5,02E-07 | 13 |
| | | sarcoma | 8,43E-06 | 60 |
| | | soft tissue sarcoma | 8,51E-06 | 42 |
| | | rhabdomyosarcoma | 1,42E-04 | 20 |
| | BM | soft tissue sarcoma | 3,00E-04 | 4 |
| **TRbp53-10Days vs wt** | BM | bone cancer | 7,64E-06 | 43 |
| | | osteosarcoma | 3,62E-05 | 30 |
| | | leiomyomatosis | 5,24E-05 | 107 |

**B**

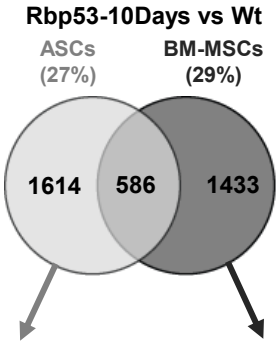


**C**

| Canonical Pathways | p-value | Canonical Pathways | p-value |
|---|---|---|---|
| Cell Cycle Control of Chromosomal Replication | 7.9E-09 | Role of Osteoblasts, Osteoclast & Chondrocytes in Rheum. Arthr. | 7.1E-06 |
| Mitotic Role of Polo-Like Kin. | 5.3E-06 | G-Protein Coupled Recep. Sign. | 1.5E-05 |
| BRCA1 in DNA Damage Resp. | 5.6E-05 | Coagulation System | 4.8E-04 |
| G2/M DNA Dam. Checkp. Reg. | 6.6E-04 | Wnt/β-catenin Signaling | 1.2E-03 |
| Mismatch Repair in Eukaryotes | 1.1E-03 | LXR/RXR Activation | 1.9E-03 |
| Aryl Hydrocarbon Recep. Sign. | 1.2E-03 | Axonal Guidance Signaling | 2.7E-03 |
| DNA DSB Repair by HR | 2.0E-03 | Embryonic Stem Cell Pluripot. | 2.9E-03 |
| Granzyme A Signaling | 5.3E-03 | cAMP-mediated signaling | 9.2E-03 |
| ATM Signaling | 7.8E-03 | MSP-RON Signaling Pathway | 1.4E-02 |
| GADD45 Signaling | 8.7E-03 | Acute Phase Response Signaling | 1.5E-02 |
| VDR/RXR Activation | 9.1E-03 | NF-κB Signaling | 2.7E-02 |
| CHK Prot. in Cell Cycle Checkp. | 1.3E-02 | Actin Cytoskeleton Signaling | 2.8E-02 |
| p53 Signaling | 1.4E-02 | Calcium Signaling | 2.8E-02 |
| G-Protein Coupled Recep. Sign. | 2.5E-02 | RhoA Signaling | 3.0E-02 |
| cAMP-mediated signaling | 4.6E-02 | BMP signaling pathway | 4.9E-02 |
| **Upstream Regulators** | **p-value** | **Upstream Regulators** | **p-value** |
| CDKN1A | 2.5E-33 | TGFB1 | 4.8E-10 |
| TP53 | 3.6E-32 | TNF | 3.9E-08 |
| E2F4 | 4.5E-31 | ERBB4 | 9.0E-08 |
| CCND1 | 1.0E-20 | KLF2 | 1.8E-07 |
| RB1 | 1.5E-20 | WNT3A | 2.3E-07 |
| EP400 | 1.5E-19 | TGFB3 | 4.4E-07 |
| CDK4 | 3.1E-19 | HGF | 8.3E-07 |
| TBX2 | 3.5E-19 | IL1B | 1.6E-06 |
| HGF | 4.0E-17 | PDGF BB | 1.8E-06 |
| CDKN2A | 2.4E-16 | HOXA10 | 6.7E-06 |

**Table S1: Sequences of primers used in the present study.**

| Gene | Forward (5´ → 3´) | Reverse (5´ → 3´) |
|---|---|---|
| ***p53*** | AAGGGGTATGAGGGACAAGG | 5-GAAGACAGAAAAGGGGAGGG |
| ***Rb*** | GGCGTGTGCCATCAATG | AACTCAAGGGAGACCTG |
| ***Collagen-type 1*** | CGAGTCACACCGAACTTGG | GCAGGCAGGGCCAATGTCTA |
| ***Osteopontin*** | TGCTTTTGCCTGTTTGGCAT | TTCTGTGGCGCAAGGAGATT |
| ***Osterix*** | GCAAGGCTTCGCATCTGAAAA | AACTTCTTCTCCCGGGTGTGA |
| ***BMP-4*** | TAAGAACTGCCGTCGCCATT | GGCCACAATCCAATCATTCC |
| ***Osteocalcin*** | CTGACCCTGGCTGCGCTCTG | GGCTGGGGACTGAGGCTCCA |
| ***β-Actin*** | GCCATCCAGGCTGTGCTGTC | TGAGGTAGTCTGTCAGGTCC |

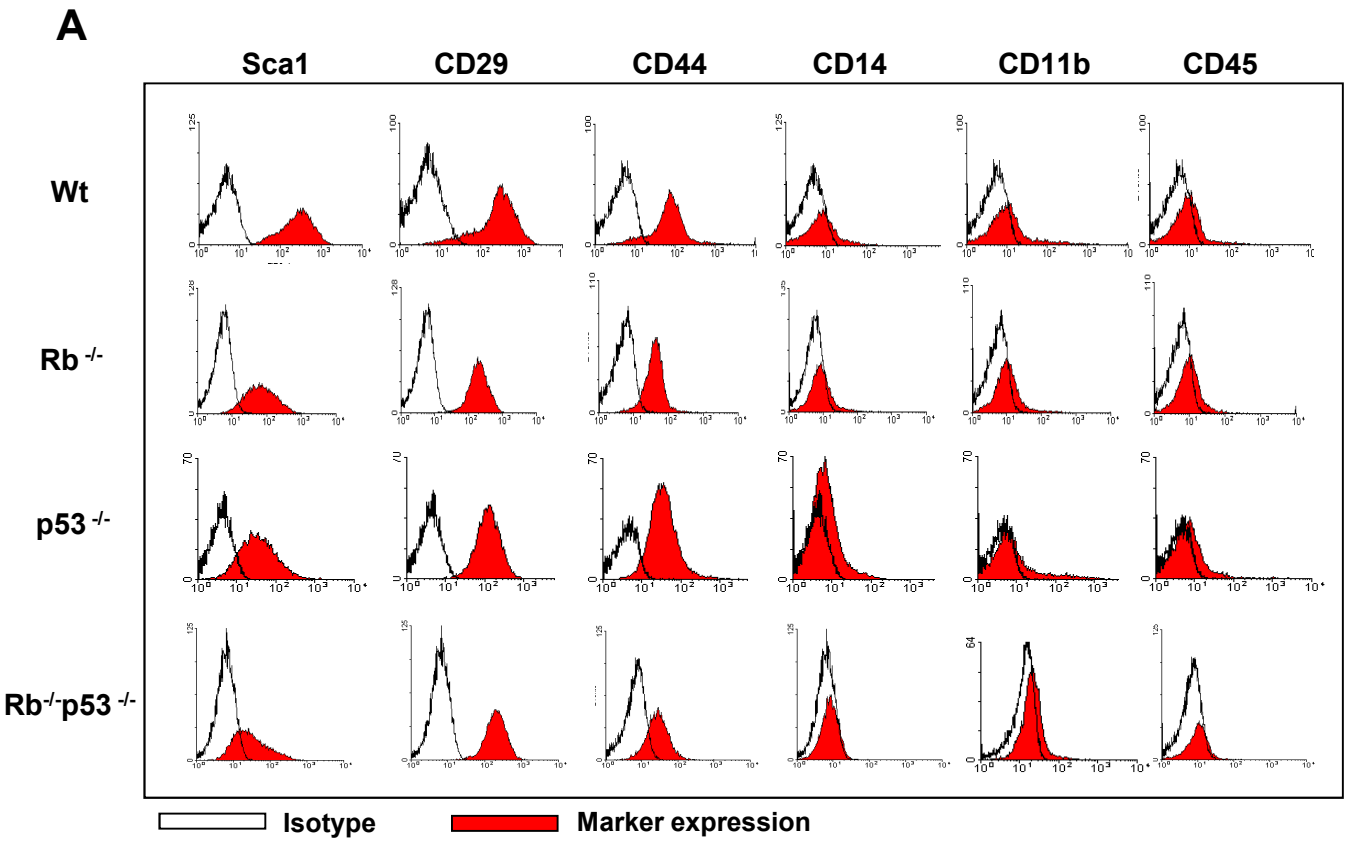


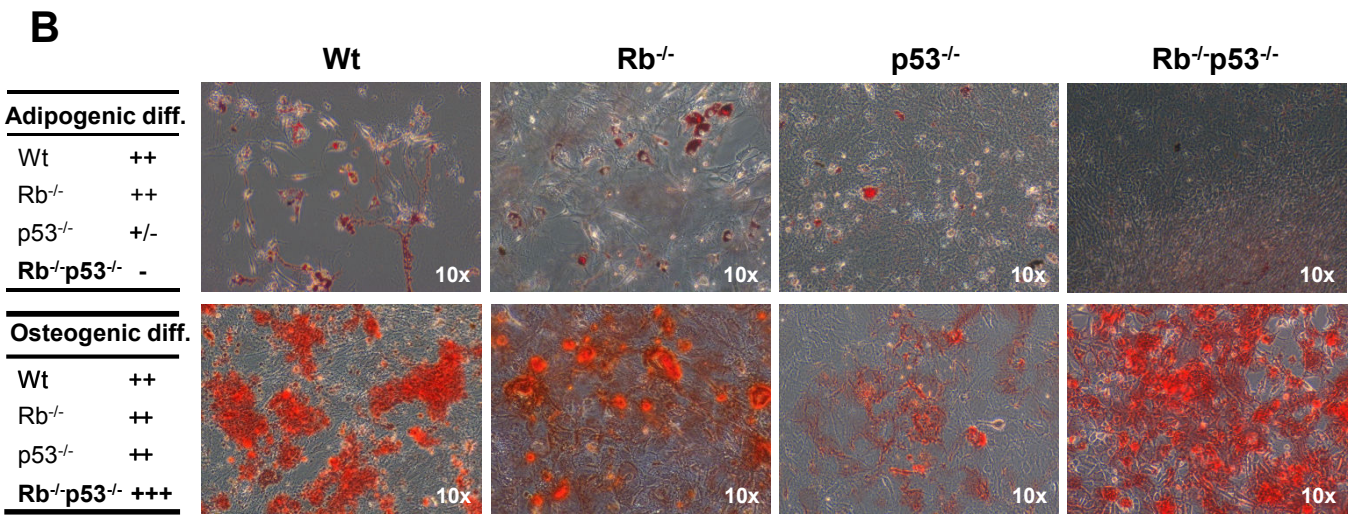


**Supplementary Figure S1. Phenotypic and functional characterization of the MSC genotypes used in the present study. (A)** Immunophenotypic profile of the indicated BM-MSC genotypes analyzed by flow cytometry. Representative dot plots are shown for Sca-1, CD29, CD44, CD14, CD11b, and CD45. Empty lines represent the irrelevant isotypes. Red-filled lines display antibody-specific staining. **(B)** Adipogenic (Oil red staining; top panels) and osteogenic (Alizarin red staining; bottom panels) differentiation potential of BM-MSCs with the distinct genotypes indicated. Original magnification is indicated.

Rubio et al. Figure S2

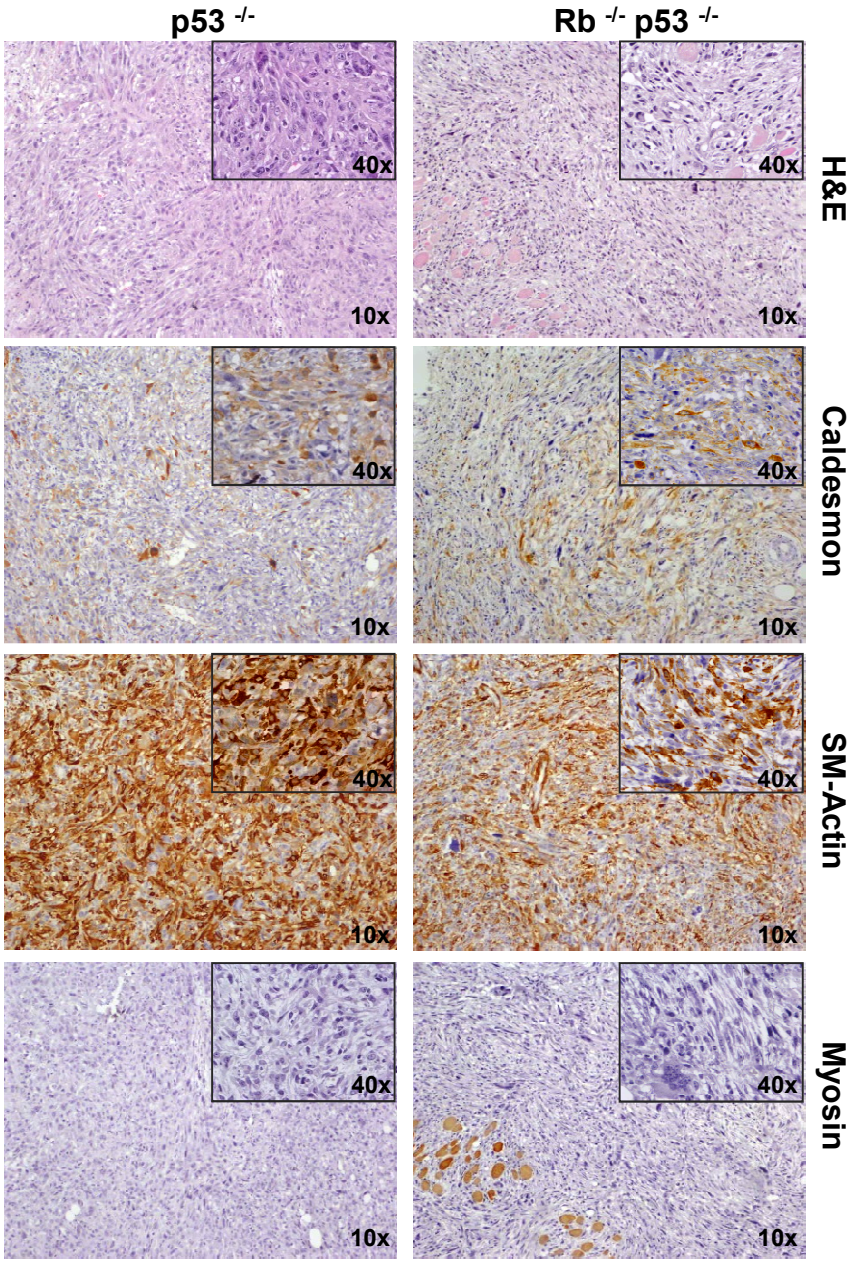


**Supplementary Figure S2. Histological analysis of tumors developed in NOD/SCID mice inoculated with p53-/- (left) and Rb-/-p53-/- (right) ASCs**. Staining is shown for H&E, caldesmon, smooth muscle actin and myosin. Insets show 40x magnification.

**Rubio et al. Figure S3**

**A**

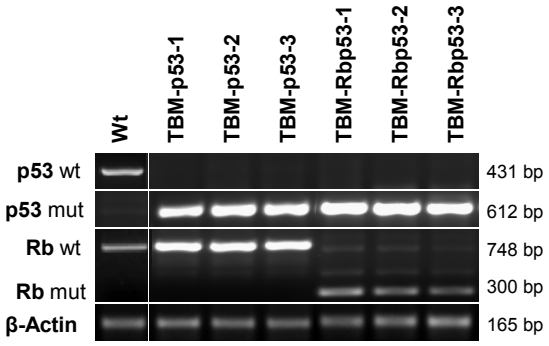


**B**

| Tumoral MSC | tumour incidence | Latency |
|---|---|---|
| TBM-p53-1 | 6/6 | 16§ |
| TBM-Rbp53-1 | 6/6 | 17§ |

§ Days for tumour development

**C**

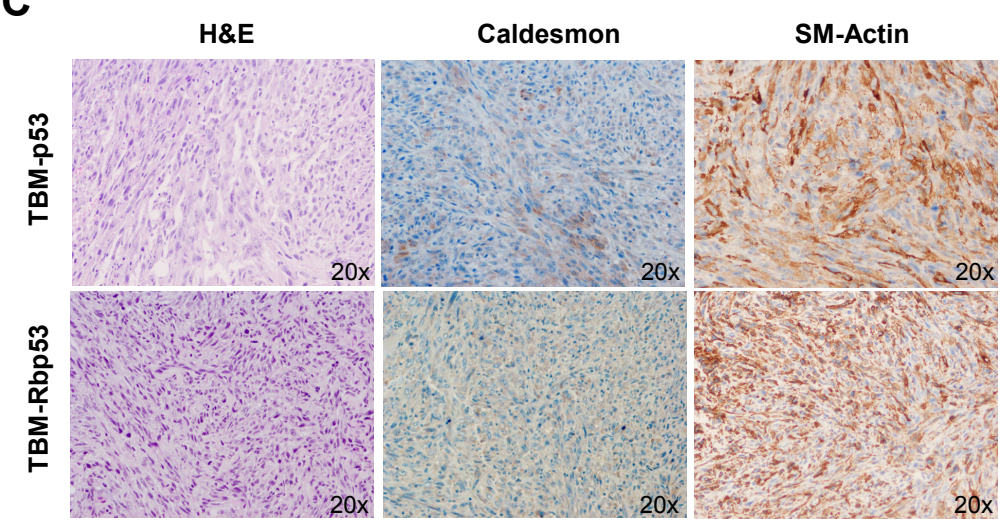


**Supplementary Figure S3. Immortalized p53-/- and Rb-/-p53-/- cell lines *ex vivo*-derived from primary tumors reinitiate sarcoma development upon secondary inoculation in NOD/SCID with 100% penetrance and much shorter latency. (A)** Tumoral cell lines *ex vivo*-derived from primary leiomyosarcomas formed by p53-/- and Rb-/-p53-/- BM-MSCs (termed Tbmp53 and TbmRbp53, respectively) retained p53 and/or Rb depletion. **(B)** *In vivo* tumor formation ability (penetrance and latency) of TBM-p53-1 and TBM-Rbp53-1 cell lines inoculated in secondary immunodeficient mice. **(C)** Representative histological analysis of secondary tumors developed in NOD/SCID mice infused with TBM-p53 and TBM-Rbp53. Staining is shown for H&E, caldesmon and smooth muscle actin. Original magnification is 20x.

| | | Sarcoma categories | p-Value | Molecules |
|---|---|---|---|---|
| p53 *vs* wt | FAT | myosarcoma | 4,68E-04 | ASS1,AURKB,CDKN1A,CDKN2A,CHEK1,FOXF1,HGF,MELK,MERTK,PBK,PFKL,PLK4,RB1,SFRP1,SKP2,TP53,TTK,VRK1,XRCC2 |
| | | sarcoma | 6,15E-04 | ASS1,AURKB,BAX,BRCA1,CCL11,CD44,CDKN1A,CDKN2A,CHEK1,FOXF1,HGF,KIF11,MDM2,MDM4,MELK,MERTK,NF2,PBK,PFKL,PLK4,RB1,SFRP1,SKP2,THBS1,TP53,TTK,VRK1,WWOX,XRCC2 |
| | | rhabdomyosarcoma | 1,01E-03 | ASS1,AURKB,CDKN1A,CDKN2A,CHEK1,FOXF1,HGF,MELK,MERTK,PBK,PFKL,PLK4,SFRP1,SKP2,TP53,TTK,VRK1,XRCC2 |
| | | tumorigenesis of muscle | 1,58E-03 | AHR,ANGPT1,CCL24,FST,HGF,IGF1R,NOS3 |
| | BM | tumorigenesis of muscle | 2,95E-04 | AHR,ANGPT1,CCL24,FST,HGF,IGF1,IGF1R,LBX1 |
| | | hyperplasia of muscle | 9,98E-04 | AHR,ANGPT1,CCL24,FST,IGF1,IGF1R,LBX1 |
| | | development of sarcoma | 7,87E-03 | BAX,HGF,IFNG,SERPINC1,TNFSF10,TP53 |
| Rbp53 *vs* wt | FAT | sarcoma | 4,44E-06 | ABAT,ABL1,ACP5,ADM,AMY2A,ASS1,BLM,BMI1,CCL11,CD44,CDH11,CDK10,CDK6,CDK7,CDKN1A,CDKN2A,CDKN2D,CHEK1,CHL1,CHRNA1,CHRNA4,CHRNG,CRABP2,DHODH,EGFR,EPHB2,ERCC2,EWSR1,FLI1,FLT1,FLT4,FNTB,FOS,FOXO1,HDAC11,HGF,IFNG,IGF1R,IL18,IL6,ITGB3,ITGB4,JUN,KDR,LCK,MCL1,MDM2,MDM4,MELK,MET,MINK1,MMP13,MUC16,MYC,MYCN,MYOCD,NCAM1,NF2,OGG1,PAX3,PDGFRB,PDPN,PINK1,PLK2,PLK4,PML,POLD1,POLE,POLE3,POPDC2,PPARG,PTCH2,PTGS2,RARB,RB1,RIPK1,RPS6KA3,SERPINC1,SFRP1,SKP2,SLC22A18,ST5,STOML2,TAOK1,THBS1,TNFRSF1B,TNFSF10,TOP2A,TP53,TTK,TUBA3C/TUBA3D,TUBA8,TUBB2A,TUBG1,TYMS,UBE2C,VEGFC,VRK1,WWOX,XRCC2,YES1 |
| | | leiomyomatosis | 2,90E-05 | ABCA8,ADARB1,AHR,AK2,ALDH1A1,ARFGEF2,ARL4D,ARNT,ASB5,ASH2L,BCL10,CAPN6,CFH,CHRDL2,COL4A6,CRABP2,CTNND1,CTSC,CXCL14,CYBA,CYP1B1,DPT,DUSP1,ECM2,EDNRB,EGFR,EIF4EBP1,EMCN,ESR1,FAS,FBLN1,FLT3LG,FOS,GPM6A,GRIA2,H19,HOPX,HSPB7,IGF1,IGF1R,IGF2,IGFBP5,ISOC1,JUN,LGR4,LIFR,LSP1,LYN,MALAT1,MEST,MET,MFAP3L,MTHFD2,MYC,MYH10,NEGR1,NOV,NSL1,OLFM1,PCCA,PDGFRB,PDK4,PGR,PIK3R3,POPDC2,PPAP2A,PPARG,PPP1R3D,PRPF8,PTTG1,RAD51L1,RAMP2,RAP2B,RAPGEF3,RGS5,RPS19,S100A4,SCARA5,SCG2,SDPR,SFRP1,SHC1,SLC24A3,SLC2A5,SLC5A3,SLC7A1,SLC7A3,SOCS3,STK25,TGFB1,TGFB3,TNC,TPBG,TWF1,UGCG,WISP2,XAF1,ZEB1 |
| | BM | myosarcoma | 2,70E-10 | ASS1,AURKB,BLM,CDKN1A,CHEK1,CNR1,CRABP2,CSF1R,DHFR,DIAPH3,FGFR1,FOXF1,FOXM1,GART,GLI2,HGF,KDR,KIT,LPPR2,MERTK,MTOR,MYCN,MYOCD,NCAM1,PBK,PFKL,PLK4,PTCH1,RB1,SKP2,SLC22A18,TK1,TOP2A,TP53,TTK,TUBB3,TUBE1,TUBG2,TYROBP,UBE2C,XRCC2 |
| | | sarcoma | 2,61E-09 | ABAT,ACP5,AMY2A,ASS1,AURKB,BLM,BRCA1,CCR5,CDH1,CDK1,CDK2,CDKN1A,CHEK1,CHL1,CHRNA1,CHRNB1,CNR1,CRABP2,CSF1R,DHFR,DIAPH3,FGFR1,FOXF1,FOXM1,GART,GLI2,HDAC11,HDAC9,HGF,HIPK2,HMMR,IL1B,IL6,ITGB3,ITGB4,KDR,KIF11,KIT,LPPR2,MDM2,MERTK,MSH2,MTOR,MYC,MYCN,MYOCD,NCAM1,NTRK3,OGG1,OSM,PBK,PDPN,PFKL,PLK4,POLA1,POLD1,POLE,POLE3,PPARG,PTCH1,RB1,SKP2,SLC22A18,THBS1,TK1,TNF,TNFRSF11A,TNFSF10,TOP2A,TP53,TTK,TUBB3,TUBE1,TUBG2,TYROBP,UBE2C,WWOX,XRCC2 |
| | | soft tissue sarcoma | 7,60E-09 | AMY2A,ASS1,AURKB,BLM,CDKN1A,CHEK1,CHL1,CNR1,CRABP2,CSF1R,DHFR,DIAPH3,FGFR1,FOXF1,FOXM1,GART,GLI2,HDAC11,HDAC9,HGF,HMMR,ITGB4,KDR,KIT,LPPR2,MERTK,MSH2,MTOR,MYCN,MYOCD,NCAM1,NTRK3,PBK,PFKL,PLK4,PPARG,PTCH1,RB1,SKP2,SLC22A18,TK1,TNF,TOP2A,TP53,TTK,TUBB3,TUBE1,TUBG2,TYROBP,UBE2C,XRCC2 |
| | | rhabdomyosarcoma | 1,76E-08 | ASS1,AURKB,BLM,CDKN1A,CHEK1,CNR1,DHFR,FOXF1,GART,GLI2,HGF,KIT,LPPR2,MERTK,MTOR,MYCN,NCAM1,PBK,PFKL,PLK4,PTCH1,SKP2,SLC22A18,TK1,TP53,TTK,TUBB3,TUBE1,TUBG2,TYROBP,XRCC2 |
| Tp53 *vs* wt | FAT | leiomyomatosis | 4,39E-07 | ADARB1,AIG1,AK2,ALDH1A1,ALDH1B1,ARFGEF2,ARL4D,ARNT,ASB5,ATRN,ATRNL1,BCL10,BDH1,CD97,CFH,CHRDL2,CLEC16A,COL4A6,CRABP2,CTNND1,CTSC,CXCL14,DLGAP4,DPT,DUSP1,ECM2,EDNRB,EGFR,EIF4EBP1,EMCN,EPPK1,ERAL1,FAS,FBLN1,FBN1,FGF2,FGFR1,FGFR3,FGFR4,FOS,GALK2,GNG11,GPM6A,GRIA2,HNMT,HOPX,HSPB7,HYAL1,IFIH1,IFIT1,IFIT3,IGF1,IGF1R,INSR,IQGAP1,ISOC1,KIT,LEFTY2,LGR4,LIFR,LSP1,LTBP1,LYN,MAF,MALAT1,MDH1,MET,MFAP3L,MLX,MMP11,MR1,MRPS23,MRVI1,MST1R,MYH10,NDRG1,NDUFV2,NOV,NSL1,NUP50,OLFM1,PDGFRA,PDGFRB,PDK4,PGR,PHLDA2,PIK3R3,PKIA,PLCB4,PLXNC1,PPAP2A,PPARG,PPP1R3D,PRPF8,PTTG1,RAB23,RAD51L1,RAMP2,RAP2B,RELA,RPE,RPS19,RPS25,RXRA,S100A4,SCARA5,SCG2,SFRP1,SHC1,SLC24A3,SLC2A5,SLC33A1,SLC5A3,SLC7A1,SLC7A3,SPSB1,STAMBP,STK25,STXBP6,TNC,TNPO3,TPBG,TSPAN12,TWF1,UBAC1,UBE2B,UGCG,VCAN,WISP2,WNT5B,WNT7A,XAF1,ZDHHC17,ZEB1 |
| | | myosarcoma | 1,44E-04 | ASS1,BLM,CDKN1A,CDKN2A,CELA1,CRABP2,DHFR,ERBB2,FGFR1,FGFR3,FLT1,FLT4,FOXF1,FOXM1,GART,HGF,IGF1R,KDR,KIT,LCK,LTK,MELK,NCAM1,PAX3,PBK,PDGFRA,PDGFRB,PIPOX,PLK2,PLK4,PTCH2,PTGS2,RB1,SFRP1,SKI,SKP2,SLC22A18,SPP1,ST5,STK24,TOP2A,TP53,TTK,TUBA3C/TUBA3D,TUBA8,TUBB2C,TUBB4,TUBG1,TYMS,TYROBP,UBE2C,VRK1,XRCC2 |
| | | leiomyosarcoma | 4,21E-04 | CDKN1A,CDKN2A,CRABP2,FGFR1,FGFR3,FLT1,FLT4,FOXM1,IGF1R,KDR,KIT,LCK,LTK,PDGFRA,PDGFRB,PTGS2,RB1,SPP1,ST5,TOP2A,TP53,UBE2C |
| | BM | myosarcoma | 1,15E-04 | CDKN1A,CELA1,CRABP2,DHFR,DIAPH3,EPHA2,FGFR3,FLT1,FLT4,FOXF1,FOXM1,GLI2,HGF,IL17B,KDR,LCK,MAP4K4,MERTK,MTOR,MYOCD,NCAM1,PBK,PLK2,PLK4,PRC1,RB1,SFRP1,SKI,SKP2,SLC22A18,TK1,TOP2A,TP53,TUBA8,TUBB2C,TUBE1,TYMS,TYROBP,UBE2C,XRCC2 |
| | | sarcoma | 3,17E-04 | BRCA1,CDH1,CDH11,CDK1,CDK6,CDKN1A,CELA1,CHL1,CHRNA1,CHRNB1,CRABP2,DHFR,DIAPH3,EGFR,EPHA2,EPHB2,ERCC2,EWSR1,FGFR3,FLT1,FLT4,FOXF1,FOXM1,GLI2,HDAC11,HDAC4,HDAC9,HGF,HIPK2,HMMR,IL17B,ITGB3,ITGB4,KDR,KIF11,LCK,MAP4K4,MDM2,MDM4,MERTK,MET,MINK1,MMP13,MSH2,MTOR,MYOCD,NCAM1,NF2,NTRK3,PBK,PINK1,PLK2,PLK4,POLD1,POLE,POLE2,POLE3,POLE4,PRC1,RAF1,RARB,RB1,RRM2,RXRA,SFRP1,SKI,SKP2,SLC22A18,STK35,STOML2,TAOK1,THBS1,THBS3,TK1,TNFRSF11A,TNFSF10,TOP2A,TP53,TUBA8,TUBB2C,TUBE1,TYMS,TYROBP,UBE2C,VEGFC,WWOX,XRCC2 |
| | | leiomyosarcoma | 5,86E-04 | CDKN1A,CRABP2,DIAPH3,FGFR3,FLT1,FLT4,FOXM1,IL17B,KDR,LCK,MTOR,MYOCD,PRC1,RB1,TOP2A,TP53,UBE2C |
| TRbp53 *vs* wt | FAT | leiomyomatosis | 6,22E-07 | ACTC1,ADAM12,AK2,ALDH1A1,ALDH1B1,ARFGEF2,ARL4D,ARNT,ASB5,ASH2L,ATRN,AURKB,BCL10,BDH1,CAPN6,CD97,CDC7,CFH,CHRDL2,CLCN5,COL4A6,CRABP2,CTNND1,CTSC,CYP1B1,DUSP1,ECM2,EDNRB,EGFR,EIF4EBP1,EMCN,ERAL1,ESR1,FAS,FBLN1,FBN1,FGFR3,FGFR4,FOS,GABBR1,GNG11,GRIA2,H19,HOPX,HSPB7,HYAL1,IFIH1,IFIT1,IFIT3,IGF1,IGF1R,LIFR,LSP1,LYN,MAF,MALAT1,MEST,MET,MFAP3L,MICALL1,MMP11,MR1,MRVI1,MYC,MYH10,NEGR1,NOV,NSL1,OLFM1,PDGFRB,PDK4,PDS5B,PEG3,PGR,PHLDA2,PIK3R3,PKIA,PLXNC1,POLR3F,PPAP2A,PPP1R3D,PPP3CB,PRPF8,PTTG1,RAD51L1,RAP2B,RPS19,RPS25,S100A4,SCARA5,SCG2,SFRP1,SHC1,SLC18A3,SLC24A3,STAMBP,STK25,STX3,STXBP6,TGFB1,TMEM59,TNC,TPBG,TSPAN12,TWF1,UBE2B,UGCG,VCAN,WISP2,WNT5B,WNT7A,XAF1,ZEB1 |
| | | sarcoma | 5,15E-05 | ABAT,ACP5,ADM,ALDH5A1,AMY2A,ASS1,AURKB,BLM,BRAF,BRCA1,CCL11,CD44,CDH1,CDK3,CDK6,CDK8,CDKN1A,CDKN2A,CDKN2D,CHRNA4,CHRNA5,CLK4,CRABP2,CUL9,DHFR,DHODH,EGFR,EPHB2,ERCC2,EWSR1,FGFR3,FLI1,FLT1,FLT4,FOS,FOXF1,FOXM1,GART,HDAC2,HDAC5,HDAC9,HGF,HIPK2,HMMR,IFNG,IGF1R,IL6,ITGAV,KDR,KIF11,LCK,LGALS3BP,MDM2,MDM4,MELK,MET,MINK1,MMP13,MTOR,MUC16,MYC,MYCN,NF2,OGG1,PAX3,PBK,PDGFRB,PDPN,PINK1,PLK2,PLK4,PML,POLA1,POLD1,POLE,POLE2,POLE3,PTCH2,PTEN,PTGS2,RARB,RB1,SERPINC1,SFRP1,SKP2,SLC22A18,ST5,STOML2,TAOK1,THBS1,TK1,TNFRSF11A,TOP1,TOP2A,TP53,TTK,TUBA8,TUBB3,TUBG1,TYMS,TYROBP,UBE2C,VRK1,WWOX,XRCC2 |
| | | myosarcoma | 1,88E-04 | ASS1,AURKB,BLM,CDKN1A,CDKN2A,CRABP2,DHFR,FGFR3,FLT1,FLT4,FOXF1,FOXM1,GART,HGF,IGF1R,KDR,LCK,MELK,MTOR,MYCN,PAX3,PBK,PDGFRB,PLK2,PLK4,PTCH2,PTEN,PTGS2,RB1,SFRP1,SKP2,SLC22A18,ST5,TK1,TOP2A,TP53,TTK,TUBA8,TUBB3,TUBG1,TYMS,TYROBP,UBE2C,VRK1,XRCC2 |
| | BM | soft tissue sarcoma | 1,63E-04 | ABL1,ADM,AMY2A,ASS1,AURKB,BAX,BLM,BRAF,CDK6,CDKN1A,CELA1,CHEK1,CSF1R,DDB2,DHFR,F2R,FGFR1,FGFR3,FKBP1A,FLT1,FLT3,FNTA,FNTB,FOXF1,FOXM1,FOXO1,GATA1,GLI2,HDAC10,HDAC11,HDAC2,HDAC5,HDAC6,HDAC9,HGF,HSP90AB1,HSP90B1,HSPA4,HYOU1,IGF1R,ITGB4,LCK,MAP4K4,MELK,MET,MSH2,MTOR,MYCN,NCAM1,NF1,NTRK3,PAX7,PBK,PDGFRA,PPARG,PRC1,PTCH1,PTCH2,PTGS2,PTPN11,RAF1,RB1,RIPK1,RNF5,SFRP1,SKI,SKP2,SLC22A18,SRC,ST5,STK24,TFAP2B,TNF,TNFRSF1B,TOP2A,TP53,TTK,TUBA1C,TUBA3C/TUBA3D,TUBB3,TUBG2,TYROBP,UBE2C,VEGFA,VRK1,XRCC2 |
| | | leiomyomatosis | 2,13E-04 | ABCA8,ACTC1,ADAM12,ADARB1,AHCYL1,AIG1,ALDH1A1,ALDH1B1,ARFGEF2,ARL4D,ARNT,ASH2L,AURKB,BCL10,C18orf1,CALCRL,CAPN6,CBL,CD97,CDC7(includesEG:12545),CFH,CLCN5,CLEC16A,CSF1R,CTSC,CXCL14,CYBA,CYP1B1,DDX24,DDX6,DLGAP4,DPT,DUSP1,EDNRB,ERAL1,ERBB4,ESR1,ESRRG,FAS,FGFR1,FGFR3,FGFR4,FLT3,FMOD,GABBR1,GNG11,H19,HNMT,HOPX,HSP90AB1,HYAL1,IFI44L,IFIH1,IGF1,IGF1R,IGF2,IGFBP5,INSR,LEFTY2,LIFR,LRCH4,LSP1,LTBP1,LYN,MAF,MALAT1,MAPK1,MAX,MDH1,MEST,MET,MFAP3L,MGST1,MICALL1,MRPS23,MRVI1,MTHFD2,MYC,MYL6,NDRG1,NDUFV2,NEGR1,NPEPPS,NSL1,NUP50,PCP4,PDE5A,PDGFRA,PDK4,PDS5B,PEG3,PHLDA2,PIK3R3,PKIA,PLCB4,PLD3,PPAP2A,PPARG,PPP1R3D,PPP3CB,PRKRIR,PSEN2,PSMC3IP,RAB23,RAB9A,RAD51L1,RAMP2,RAP2B,RAPGEF3,RELA,RGS5,RPL27,RPS25,S100A4,SCARA5,SEC22B,SF3A1,SFRP1,SHC1,SLC24A3,SLC2A5,SLC5A3,SLC7A3,SMAD5,SOX4,SPSB1,STAMBP,STXBP6,TBL1X,TNC,TNPO3,TPBG,TSPAN12,UBE2B,UGCG,UNC5D,VCAN,WNT5B,XAF1,ZDHHC17,ZEB1,ZNF148 |

**Supplementary Figure S4.** Complete list of genes associated to sarcoma differentially expressed (p value<0.05; expression >2-fold up or down) in p53-/- and Rb-/-p53-/- ASC/BM-MSC and their derived tumors Tp53 and TRbp53 as compared to wt-ASC/BM-MSC (see Figure 2A).

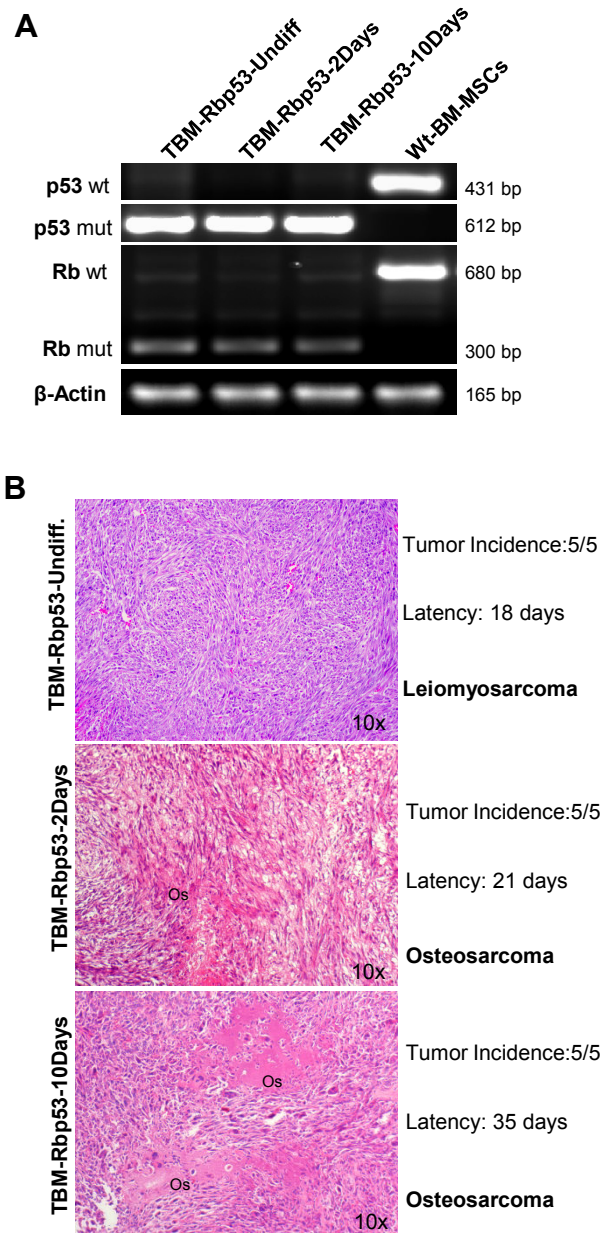


**Figure S5. Immortalized Rb-/-p53-/- cell lines *ex vivo*-derived from primary tumors reproduce osteosarcoma development upon secondary inoculation in NOD/SCID with 100% penetrance and much shorter latency. (A)** Tumoral cell lines *ex vivo*-derived from primary sarcomas formed by either Rb-/-p53-/- undifferentiated BM-MSCs (TBM-Rbp53-Undiff) or Rb-/-p53-/- BM-MSC-derived osteogenic progenitors (TBM-Rbp53-2Days and TBM-Rbp53-10Days) retained p53 and Rb depletion. **(B)** Tumor incidence, latency and histological analysis (H&E staining, 10x original magnification; Os: osteoid matrix) of secondary tumors developed in NOD/SCID mice inoculated with TBM-Rbp53-Undiff (top), TBM-Rbp53-2Days (middle) and TBM-Rbp53-10Days (bottom) cell lines.

| | | Sarcoma categories | p-Value | Molecules |
|---|---|---|---|---|
| Rbp53-D10 *vs* wt | ASC | myosarcoma | 1,64E-08 | ASS1,BLM,CDKN1A,CKS2,DIAPH3,FOS,FOXM1,FOXO1,GLI1,HRAS,MELK,MYOCD,PBK,PLK4,PRC1 ,PSMB9,PTGS2, RB1,SKP2 (includes EG:27401),SLC22A18,SPHK1,SPP1,TK1,TOP2A,TP53,TTK,TUBB3,TUBE1,UBE2C,VRK1,XRCC2 |
| | | leiomyosarcoma | 5,02E-07 | CDKN1A,CKS2,DIAPH3,FOXM1,MYOCD,PRC1 (includes EG:233406),PSMB9,PTGS2,RB1,SPP1,TOP2A, TP53 (includes EG:22059),UBE2C |
| | | sarcoma | 8,43E-06 | ANGPTL4,ASS1,BAX,BLM,BRCA1,CCL11,CDKN1A,CKS2,CYP1B1,DHFR,DIAPH3,EDN1,FLI1,FLT1,FOS,FOXM1, FOXO1,GLI1,GSTM3,H2AFX,HMMR,HRAS,HSPA4,IFNG,IGFBP5,IL5,IL6,KIF11,LCK,MDM2,MELK,MMP13,MMP9, MYOCD,PBK,PDK4,PLK4,PRC1 (includes EG:233406),PSMB9,PTGS2,RARB,RB1,RECQL4,RUNX1T1,SKP2 (includes EG:27401),SLC22A18,SPHK1,SPP1,SSBP2,SSTR2,THBS1,TK1,TOP2A,TP53,TTK,TUBB3,TUBE1,UBE2C,VRK1,XRCC2 |
| | | soft tissue sarcoma | 8,51E-06 | ASS1,BAX,BLM,CCL11,CDKN1A,CKS2,DIAPH3,FLT1,FOS,FOXM1,FOXO1,GLI1,HMMR,HRAS,HSPA4,IFNG (includes EG:15978),IL5,LCK,MELK,MMP13,MYOCD,PBK,PDK4,PLK4,PRC1 ,PSMB9,PTGS2,RB1,SKP2,SLC22A18,SPHK1, SPP1,THBS1,TK1,TOP2A,TP53 (includes EG:22059),TTK,TUBB3,TUBE1,UBE2C,VRK1,XRCC2 |
| | | rhabdomyosarcoma | 1,42E-04 | ASS1,BLM,CDKN1A,FOS,FOXO1,GLI1,HRAS,MELK,PBK,PLK4,SKP2 (includes EG:27401),SLC22A18,SPHK1,TK1, TP53,TTK,TUBB3,TUBE1,VRK1,XRCC2 |
| | BM | soft tissue sarcoma | 3,00E-04 | CDKN2A,HGF,NT5E,TP53 (includes EG:22059) |
| TRbp53-10Days *vs* wt | BM | bone cancer | 7,64E-06 | ACP5,ALK,BAX,BCL2L1,CACNA2D1,CACNA2D2,CAT,CD44,CDH11,CDKN1A,CDKN2A,CDKN2B,CHEK2,DHFR, EDN1,FLI1,FOS,GLI1,GLI2,GSTM3,IFITM2,IGFBP5,IL6,JUN,LOXL2,MMP9,MSH2,MYC,NPM1,NRAS,PLAU, PLAUR,PTEN,RB1,SDC2,SERPINE1,SMO,SPARC,SPP1 (includes EG:100359743),THBS1,TIMP1,TP53,TP63 |
| | | osteosarcoma | 3,62E-05 | ACP5,BAX,CD44,CDH11,CDKN2A,CDKN2B,CHEK2,DHFR,EDN1,FLI1,FOS,GLI1,GLI2,GSTM3,IFITM2,IGFBP5, JUN,MMP9,MSH2,NRAS (includes EG:18176),PTEN,RB1,SDC2,SMO,SPARC,SPP1,THBS1,TIMP1,TP53,TP63 |
| | | leiomyomatosis | 5,24E-05 | ABCA8,ADAM12,ADARB1,AHCYL1,AHR,AIG1,ALDH1A1,ALDH1B1,ARFGEF2,ARNT,ASH2L,ATRNL1,C18orf1, CAPN6,CD97,CDC7,CFH,CSF1R,CTNND1,CTSC,CXCL14,CYBA,CYP1B1,DOK1,DPT,DUSP1,DVL1,ECM2,EGFR, EIF4EBP1,ESR1,FAS,FBLN1,FBN1,FGF2,FGFR2,FGFR3,FGFR4,FMOD,FOS,GALK2,GNG11,GUCY1A2,H19,HMGA2, HNMT,HOPX,HSPB7,IFNAR1,IGF1,IGF2,IGFBP5,INSR,ISOC1,JUN,KCNG1,LIFR,LTBP1,MAOA,MEST,MET,MFAP3L, MGST1,MRVI1,MST1R,MTHFD2,MYC,MYL6,NEGR1,NOV,OLFM1,PCP4,PDGFRA,PDK4,PHLDA2,PIK3R3,PLCB4,PLD3, PPAP2A,PPARG,PPP1R3D,PSEN2,PTTG1,RAD51B,RAMP2,RAP2B,RAPGEF3,RXRA,SCARA5,SCG2,SDPR,SFRP1, SLC24A3,SLC2A5,SLC5A3,SLC7A3,SMAD5,SORBS2,SPSB1,STX3,STXBP6,TNC,UBAC1,VCAN,WISP2,XAF1,ZYX |

**Supplementary Figure S6.** Complete list of genes associated to sarcoma differentially expressed (p value<0.05; expression >2-fold up or down) in ASC-Rbp53-10Days, BM-Rbp53-10Days and TBM-Rbp53-10Days cells as compared to wt-ASC/BM-MSC (see Figure 5A).